Resilient Provision of Ecosystem Services from Agricultural Landscapes: Tradeoffs Involving Means and Variances of Water Quality Improvements

ABSTRACT

We assess the tradeoffs and synergies involved in reducing agriculture-generated nutrient loads with different levels of resilience. We optimize the selection of least-cost patterns of agricultural conservation practices for both the expected performance of the conservation actions and its variance. Securing nutrient loads with a higher level of resilience is costly, with marginal costs of resilience generally declining with lower loads. We find that the main tradeoff dimension is between cost of conservation investments and ecosystem service objectives, as opposed to pronounced mean-variance or between- nutrient objectives tradeoffs. We find relative synergies in agricultural conservation investments aimed at nutrient reductions.

Keywords: *agricultural conservation practices, agricultural nonpoint-source pollution, ecosystem services tradeoffs; multiobjective optimization; evolutionary algorithms, safety-first; resilience*

JEL Codes: Q25, C63

Suggested running head: Resilient Provision of Water Quality from Agriculture

Sergey Rabotyagov (corresponding author),
Associate Professor
School of Environmental and Forest Sciences,
Box 352100,
University of Washington, Seattle WA 98195-2100
Tel: 515-451-7218
Fax: 206-685-0790
E-mail: *rabotyag@uw.edu*

Adriana Valcu
Postdoctoral Research Associate
Center for Agricultural and Rural Development
Department of Economics
Iowa State University, Ames, IA

Catherine L. Kling
Director and Charles F. Curtiss Distinguished Professor
Center for Agricultural and Rural Development
Department of Economics
Iowa State University, Ames, IA

Acknowledgments

This research was funded in part from support received from the National Science Foundation's Water, Sustainability, and Climate program joint with National Institute of Food and Agriculture (#NSF-WSC 1209402 and WNZ-A71219) and two awards from the National Institute of Food and Agriculture (#2014-51130-22494 and 2011-68002-30190). We thank Todd Campbell, Phil Gassman, and Yongjie Ji for technical assistance and helpful suggestions. All errors remain our sole responsibility.

Resilient Provision of Ecosystem Services from Agricultural Landscapes: Tradeoffs Involving Means and Variances of Water Quality Improvements

In recent years, the concept of ecosystem services and natural capital has garnered significant attention from the research, policy, and conservation community (see, e.g., Heal and Small (2002), Boyd and Banzhaf (2007), Polasky and Segerson (2009), Barbier (2015), and a Special Feature in the *Proceedings of National Academy of Sciences* devoted to the topic). For intensively managed agriculture-dominated landscapes, there can be both complementarities and competition between ecosystem services including the provisioning services of food, feed, fuel, and clean water, the regulating service of waste processing (provided by streams), and the cultural ecosystem services tied to the presence of wildlife for hunting or recreation. The diminution of ecosystem services related to environmental externalities is, of course, a generally expected outcome of a market system. Given the signals provided by agricultural markets, it is not surprising that the agricultural system heavily favors production of private ecosystem services (food, feed, and fuel) (Lichtenberg 2002, p. 1254). The US Midwest, for example, has the highest rates of crop growth in the world, to the point that agriculture affects regional climate (Mueller et al. 2015). At the same time, heavy reliance on fertilizer use, has caused some scientists to suggest that humanity has exceeded its "safe operating space" with respect to nutrient fluxes (Steffen et al. 2015).

The recognition of these issues has led to extensive agri-environmental policy efforts in the US and elsewhere as well as a literature identifying approaches for incorporating ecological objectives in policy (Lichtenberg 2002; Lankoski and Ollikainen 2003, Bateman et al. 2013). While these efforts have found some success, most scientific assessments of environmental impacts of U.S. agriculture indicate many remaining concerns including fish and wildlife habitat

(USDA-CEAP, Wildlife National Assessment 2015), air pollution (Mueller and Mendelsohn 2011), nutrient pollution (US EPA 2015), and other environmental endpoints.

Elucidating the nature of tradeoffs between different ecosystem services requires understanding natural system processes and evaluating *counterfactual* scenarios to determine where tradeoffs exist, where synergies occur (e.g., Karp et al. 2015), and how other ecosystem services can be improved at the lowest sacrifice to marketed agricultural goods. Understanding tradeoffs or potential synergies[1] requires two things. First is the quantifiable understanding of the underlying ecosystem service production process and of the economic inputs that go into their production.[2] The ecological production functions themselves, however, are often poorly understood, may exhibit complex nonlinear dynamics with thresholds (e.g., Carpenter et al. 2015; Barbier et al. 2008), or, even in the best case of relatively small scientific uncertainty, may be represented by computer simulation programs that do not correspond to traditional economics understanding of a production function (e.g., Heal and Small 2002).

While tradeoffs in ecosystem services may be unavoidable, it is desirable to limit consideration to those that are on a Pareto-efficient frontier. This is particularly important when considering the exact magnitudes (marginal costs or marginal rates of product transformation) of tradeoffs between ecosystem services. Yet another dimension to the question of tradeoffs between different classes of ecosystem services is uncertainty in the provision of a particular joint product from an ecosystem. In addition to having different opportunity costs of private goods, alternative ecosystem service bundle can differ in terms of the risk associated with their

[1] Heal et al. (2001) called the presence of synergies a "conservation umbrella."

[2] See Heal and Small (2002) for an interesting distinction between economic and non-economic inputs into the ecosystem services production function. Economic inputs have opportunity costs, while others, like sunlight needed for agricultural production, while essential, are non-economic In our application, economic inputs include foregoing crop production entirely and planting perennial grass or bringing machinery, expertise, and labor inputs for the adoption of "working land" conservation practices.

provision. That is, some conservation investments may consistently yield a given bundle of ecosystem services while others may on average a higher level of services, but with a wider variability of provision over time. The mean-variance tradeoff for a particular cost of conservation investment may be relevant in choosing across services.

Consideration of tradeoffs between mean and variance of provision of services is consistent with the literature on resilience in ecosystem service provision. The notion of resilience is nuanced and complex, but for this work we adopt a definition similar to one used in Gren (2010) —namely, the reliability of ecosystem service provision under exogenous shocks, specifically weather risk.[3] In this paper, we explore tradeoffs for the expected provision level and for different levels of reliability (specified as simulated probability of attaining the desired provision level) for the case of a single non-market ecosystem service, and then expand the notion of tradeoffs to multiple dimensions of aquatic ecosystem services, where we focus on the joint probability of meeting desired ecological targets.[4] To do so, we adopt a multiobjective optimization approach with the objectives specified as means and standard deviations of desired ecosystem outputs. For this application, we focus on a heavily agricultural watershed in Iowa and use nutrient loads as inputs into aquatic ecosystem services. This approach can will be relevant to any situation where the connection between human actions on the landscape and ecosystem services is characterized by a complex relationship involving nonlinearities, nonconvexities and nonseparabilities (for example, conservation network design as in Parkhurst and Shogren 2008).

[3] Social preference for reliability of goal attainment is reflected in the required "margin of safety" in the TMDL regulations, requiring either to explicitly reduce allowable pollutant loads in a watershed based on modeled uncertainty or to employ conservative modeling assumptions (http://water.epa.gov/lawsregs/lawsguidance/cwa/tmdl/TMDL-ch3.cfm)

[4] However, as Heal and Small (2002) point out "We are powerfully ignorant about the technology that produces ecosystem services." While true, ignorance should not be a reason to explore the implications of existing levels of understanding of some dimensions of ecosystem services production process, embodied, in our case, in the ecohydrologic model. See Kling (2011) for a call to action while acknowledging the deep uncertainties involved and importance of learning and adaptive management.

.

Resilience in ecosystem services provision

The concept of resilience has been used extensively by many disciplines, each approaching the concept from somewhat different perspectives and providing different definitions. We refer the reader to Longstaff et al.'s (2013) typology and to translate the concept among different disciplines. Intuitively, the notion of resilience deals with the ability of a system to perform desired functions under most, if not all, possible external shocks. Within their typology, we adopt the definition referred to as Type I resilience: the capacity of a system "to rebound and recover." Simply put, we seek to spatially optimize the selection of agricultural conservation practices which optimize both the expected performance of the conservation actions and their variance (Shortle and Horan (2013) suggest a similar approach). Longstaff et al's (2013) typology distinguishes approaches to resilience based on level of complexity (low/reductionist approach to high/holism/emergent properties) of the studied system as well as based on degree of normativity (on the scale from descriptive/positive to normative). Our work fits in the low complexity/low normativity category, as our studied system deals with quantifiable uncertainty (risk) and employs a deterministic, reductionist approach to quantifying the costs and ecosystem service outputs of evaluated scenarios.[5] This definition of resilience can be equivalently thought of as the reliability of meeting ecosystem service provision targets.

Next, we briefly sketch a simple model to aid in conceptual framing of our work. Suppose one possesses a quantified joint ecological-economic production function $S(\boldsymbol{x};\boldsymbol{\varepsilon})$: $\mathbb{R}^{\boldsymbol{m}} \rightarrow \mathbb{R}^{\boldsymbol{k}}$, where $\boldsymbol{x}$ is an $m \times 1$ vector of controllable economic inputs into the

[5] Were we to adopt a specific form for an economic damage function associated with ecosystem service degradation, our work would align with type II resilience definition of Longstaff et al. (2013), and would involve objectives of net benefit optimization (see Polasky and Segerson (2009) and Shortle and Horan (2013) for discussion of the relationship between outcomes obtained under physically defined goals and economically efficient outcomes).

production of ecosystem services (e.g., land, machinery, labor, fertilizer input, conservation practices) being combined, over the relevant spatial and temporal scale, to produce a $k \times 1$ vector of monetized benefits/costs and nonmonetized final ecosystem services, and $\boldsymbol{\varepsilon}$ representing exogenous factors (e.g., non-economic inputs into production of ecosystem services such as rainfall, solar radiation, soil quality, as well as exogenous economic factors such as commodity prices or government policy) treated as random. One of the components of the output vector serves to monetize the choices made with respect to human actions $\boldsymbol{x}$ in the form of net social benefits. Depending on the availability of data and models, this can range from a full accounting of net social benefits measuring welfare impacts of marketed ecosystem services and non-market values of some non-market ecosystem services to simply measuring estimated engineering costs associated with $\boldsymbol{x}$. With this resilience measure, it is assumed that decision-makers can specify a set of desirable performance targets $\bar{S}$. Appropriately scaling outputs so that they are all desirable, the problem of resilience can be written as $\max_{\boldsymbol{x}} P(S(\boldsymbol{x};\boldsymbol{\varepsilon}) \geq \bar{S})$, that is, the most resilient set of actions are those that maximize the probability of meeting a desired level of monetized and non-monetized ecosystem services.

This is a version of Roy's (1952) safety-first criterion.[6] Safety-first approaches have found numerous applications in many fields, including agricultural and environmental economics. Of many past efforts, examples include Paris (1979), Beavis and Walker (1983), Lichtenberg and Zilberman (1988), McSweeny and Shortle (1990), Bigman (1996), Willis and Whittlesey (1998), Horan and Shortle (2011), Eloffson (2003), Gren (2008), Kampas and White (2003), Rabotyagov (2010). As highlighted by Shortle and Horan (2013), the Total Maximum

[6] More broadly, this kind of formulation can be described as a P-model of Chance-Constrained Programming (CCP) of Charnes and Cooper (1959), and CCP can be described as a class of anticipative (non-adaptive) stochastic programming approaches (Poojari and Varghese 2008)

Daily Load rules adopts safety-first approach through the requirement of a "margin of safety" constraint on the allowable watershed pollution loads. Another example is that the government of Canada was at one point explicitly favoring climate change policy requiring 95% certainty in agricultural carbon sequestration credits (Rabotyagov 2010).

In many applications, the tradeoffs embedded in resilience can be appropriately formulated by minimizing the (non-stochastic) cost of achieving a single stochastic ecosystem service objective with a given probability. The resilience objective is typically written as a constraint $P(S_i(\boldsymbol{x};\boldsymbol{\varepsilon}) \geq \bar{S_i}) \geq \alpha$, where α is level of resilience (or reliability) of the system. Rewriting the probabilistic constraint in a deterministic form can be accomplished when the distribution of the random term is known. In this case, a deterministic constraint involving the critical value of the standardized distribution of S_i, the controlled mean and variance of ecosystem service provision can be written as $E_\varepsilon\big(S_i(\boldsymbol{x})\big) + F_z^{-1}(1-\alpha)Var\big(S_i(\boldsymbol{x})\big)^{0.5} \geq \bar{S_i}$. For high desired levels of confidence α (so that $F_z^{-1}(1-\alpha) < 0$), the term ($F_z^{-1}(1-\alpha)Var\big(S_i(\boldsymbol{x})\big)^{0.5}$) has the standard interpretation of a "margin of safety" or of an "uncertainty discount". Tradeoffs between costs and the resilience of providing non-monetized ecosystem services are then seen by increasing cost of attaining higher reliability. This is a standard finding, although the costs of resilience have varied from single-digit percentage uncertainty discounts for soil carbon sequestration (Rabotyagov 2010), to almost doubling the costs of pollution reduction when required confidence in pollution reduction goes from 50 to 90-95% (Bÿstrom, Andersson, Gren (2000); Elofsson (2003)) to finding a seven-fold increase in costs of controlling N runoff (McSweeny and Shortle, 1990). Resilience is costly, but the exact tradeoffs involved in achieving higher resilience depends on the particular situation.[7]

[7] An obvious source of affecting costs of resilience lies with the choice of the critical value $F_z^{-1}(1-\alpha)$. Under uncertainty about the form of the controlled distribution, one can purchase resilience with respect to distributional

The simple case of no uncertainty in the opportunity costs of ecosystem services provision allows for a particularly convenient inversion of the probability statement and for dealing with "resilient" levels of provision. If $\boldsymbol{x}$ is costly, the constraint will be binding and $E_{\varepsilon}\left(S_i(\boldsymbol{x}^*)\right) + F_z^{-1}(1-\alpha)Var\left(S_i(\boldsymbol{x}^*)\right)^{0.5} = \bar{S}_i$ represents the α-quantile of the controlled provision distribution (also sometimes referred to as a claimable amount (Kurkalova 2005)) and $\boldsymbol{x}^*$ denotes choices leading to resilient provision. When multiple objectives are brought under the joint probabilistic constraint, such an inversion from joint probabilities to unique quantiles is no longer possible, except for the case of statistically independent objectives, where the jointly α^n-resilient set is constructed of individual (marginal) α-resilient provision levels. Instead, combinations of individual provision levels which jointly produce the desired α-level resilience will be required. This is akin to confidence ellipses encountered in joint significance testing of regression parameters (for the introduction to the issues encountered in joint chance constraints, see Bawa (1973), Prekopa (1970), Willis and Whittlesey (1998) for an applied agricultural economics example or Hong, Yang, and Zhang (2011) for the modern operations research perspective). In short, a simple interpretation of results as producing unique "resilient" $\bar{S}_i$, $\bar{S}_k$ no longer applies.

Fortunately, if we ask "what is the joint resilience associated with a particular solution $\boldsymbol{x}$ and specified objectives, $\bar{S}$?", the answer, expressed as a joint probability, is easy to understand (if not necessarily compute). Namely, the probability is $P(\boldsymbol{x}) = \int I[S(\boldsymbol{x};\boldsymbol{\varepsilon}) \geq \bar{S}]dF(\varepsilon)$. In some simpler cases, where a single stochastic objective is encountered, and a particular distribution for the random factor (e.g., normal) is assumed, the probability can be retrieved from existing tables. In other cases of intermediate difficulty, in which a low-dimension economic-ecological

uncertainty by relying on the Chebyschev Inequality (e.g., Gren (2010)). This, however, appears unnecessarily conservative for most practical applications.

production process may be assumed to be linear and separable ($S(\boldsymbol{x};\boldsymbol{\varepsilon}) \equiv \boldsymbol{s}(\boldsymbol{\varepsilon})'\boldsymbol{x}$), analytical expressions can be constructed (e.g., (Kampas and White 2003). However, even for a single dimension of ecosystem service output, where the production process may take place over K locations, and where multiple actions (J) are available in $\boldsymbol{x}$, construction of (conditional on $\boldsymbol{x}$) variance to arrive at the standardized ecosystem output involves estimating $\frac{KJ(KJ-1)}{2}$ terms of the variance-covariance matrix, which would account for all the spatial and action-related covariances. This is a common problem that arises in risk management, and analytical techniques such as copula estimation exist to aid researchers and decision-makers (Cherubini, Luciano, and Vecchiato, 2004).

Gren (2010) considered several abatement actions and the implied abatement correlations across actions in estimating the resilience value of wetlands for nutrient reduction; however, her analysis did not incorporate spatial correlations, while Kampas and White (2003) have shown that ignoring correlations introduces larger bias in probabilistic constraints than incorrect distribution specification. Rabotyagov (2010) considered two agricultural conservation actions as well as spatial correlation for soil carbon sequestration. However, the introduction of multiple dimensions as well as distributional assumptions needed to make probability statements further complicate the issue. For instance, Kampas and Adamidis (2005) pointed out that under log-normality assumption of pollution reduction from a single action, the sum of reductions does not follow the log-normal distribution as Gren, Destouni, and Tempone (2002) assumed.

When, in addition, the natural science knowledge suggests that important dimensions of $S(\boldsymbol{x};\boldsymbol{\varepsilon})$ are nonlinear and nonseparable (e.g., examples provided in Carpenter et al. 2015), obtaining analytical expressions for the overall resilience value becomes much more difficult. However, as in simulation-aided econometric estimation, simulation approximation to the probability or other expected functions of interest such as the mean or the variance remains

available. One issue that arises in this context is computational cost associated with evaluating $S(\boldsymbol{x};\boldsymbol{\varepsilon})$ many times. For example, we could build the objective of resilience directly into the multiobjective tradeoff analysis (see Rabotyagov, Jha, and Campbell 2010) but instead we choose to opt to formulate the objectives in terms of means and standard deviations. Resilience is a property associated with a particular choice of actions to affect the provision of a vector of desirable outputs. Basic theory and empirical work to date suggest that resilience is costly. Resilience of the type we study is closely related to the variance in the desired output. To explore the potential tradeoffs among cost and proxies for aquatic ecosystem services, as well as evaluate potential synergies or tradeoffs associated with resilience, we choose to simultaneously optimize for the cost of economic inputs, and the mean and the variance of non-market ecosystem outputs. Further, we use bootstrap methods for a computationally fast way to provide resilience assessment of the optimized solutions.

Tradeoff Development

An efficient tradeoff frontier in the production of ecosystem services emerges when all Pareto-improvements have been exhausted: no single objective can be improved upon without sacrifice in terms of other objective(s). Some of the objectives may be formulated as resilience objectives. The classic example is tracing out the efficient mean-variance frontier of a stock portfolio. For multiple objectives when the economic-ecological production function can be explicitly written exact multiobjective optimization can generate tradeoffs across different ecosystem services (see Polasky et al. (2008) and Toth and McDill (2009)). In the case that $S(\boldsymbol{x};\boldsymbol{\varepsilon})$ function is cannot be written in a compact mathematical form but is represented by a computer simulation program, simulation-optimization methods can be used.

Multiobjective evolutionary algorithms are capable of dealing with potential non-convexities in optimization and can use simulation model output to (approximately) develop multiple-

objective Pareto-efficient sets in a single optimization run. Deb (2001) is the classic introduction to evolutionary algorithms. Nicklow et al. (2010) and Maier et al. (2015) discuss some recent applications focused on water resources, and Kennedy et al (2008) and Porto et al (2014) provide terrestrial ecosystem management examples. Herman et al. (2014) explore tradeoff generation under deep uncertainty. Recent examples for tradeoff development using multiobjective evolutionary algorithms in agriculturally dominated ecosystems include Gramig et al. (2013), Bostian et al. (2015), Ahmadi et al. (2013), Rabotyagov et al. (2014) and Chichakly et al. (2013) who incorporate measures of resilience to anticipated climate change.

We consider a model of joint economic-ecological production process, where the human actions considered are "working land" agricultural conservation practices largely consistent with the prevailing crop system and "land retirement" of establishing perennial grass cover on cropland. These actions represent economic inputs into the production of (proxies for) freshwater and coastal aquatic ecosystem services associated with reducing nutrient fluxes, namely ambient Nitrogen (N) and Phosphorus (P) loads.

Scientific consensus exists on the fact that human activity has altered both the nitrogen and phosphorus cycles (Millenium Ecosystem Assessment, 2005, Ch. 12), with some beneficial (increased crop production), and some deleterious (eutrophication) effects on ecosystem services. The exact targets for nutrient loads and concentrations are an active area of research and policymaking (Evans-White et al., (2013), Heiskary and Bouchard (2015), US EPA, 2015 http://cfpub.epa.gov/wqsits/nnc-development/) but it is well understood that excess nutrient loads negatively impact many ecosystem services from freshwater systems. We take as a starting point that it is desirable to reduce N and P and elucidate the tradeoffs involved in controlling the mean and standard deviation of nutrient pollution.

Conceptual Model

Our notation is similar to the notation used by Rabotyagov, Valcu, and Kling (2014). There are K decision-making units ("fields") in the watershed, each field being characterized by a unique combination of physical characteristics (soil, slope) and location in the watershed. The ambient water quality is monitored both in stream and at the outlet of the watershed. Let $r_i = r_i(\mathbf{x_i}, \xi)\ \forall\ i = 1, \ldots, K$ be the i^{th} field emissions given the actions taken at field level, where $\mathbf{x}_i$ represents the $J \times 1$ vector of actions implemented at each field, and ξ represents the stochastic weather factor. The set of actions consists of baseline activity and a set of working land conservation practices and land retirement.

To connect farm-level conservation actions to outcomes of interest, we need a specific version of the ecological production function. In our application, this function is represented by a water quality production function, $\mathrm{W}(\mathbf{r}(\mathbf{x}, \boldsymbol{\xi}))$ that is the result of the complex spatial interactions between the edge-of-field emissions leaving the fields, and which is represented by an ecohydrologic simulation model.[8] Given the stochastic nature of the weather factor, we are interested in finding the least-cost spatial combinations **x** that reduce expected values of nutrient pollution as well as its standard deviation. Using optimization results, we construct a measure of resilience defined as the probability of achieving a particular target, and analyze the tradeoff between costs and different levels of resilience. We start by considering the case of a single nutrient pollutant (a proxy for diminished aquatic ecosystem services upstream and downstream) and then move to the case of two pollutants.

[8] As Lichtenberg (2002) explains: "… there is not a simple monotonic relationship between emissions at the level of an individual field and impacts on environmental quality at the ambient scale with which policy is actually concerned. Fate and transport are typically non-linear and depend on space and time in complex ways, making extrapolation of field-level emissions to ambient pollutant concentrations quite complex". We refer the reader to Lichtenberg (2013), Shortle and Horan (2013) for reviews of these and other issues associated with nonpoint source pollution from agriculture, as well as to Rabotyagov et al (2014) for an attempt to simplify the 'ecological production' process. Uncertainty in the model structure itself is not considered in this article, although we recognize this as likely important for both better science and policy-relevance (see Herman et al. 2014).

A single pollutant case

We begin by solving the multi-objective problem that simultaneously minimizes

$$Min_{\mathbf{x}}\left[\, C(\mathbf{x}),\ E_T[N(\mathbf{x})]\,, Var[N(\mathbf{x})]^{0.5}\right] \quad (1)$$

where $\mathbf{x}$ represents a $KJ \times 1$ vector representing a particular placement of conservation practices, $\mathrm{W}\big(\mathbf{r}(\mathbf{x},\boldsymbol{\xi})\big) \equiv N(\mathbf{x})$ represents the simulated, over simulation period of length T, vector of annual nitrogen loads, $E_T[N(\mathbf{x})]$ is the mean nitrogen loads over the historical simulation period, $Var[N(\mathbf{x})]^{0.5}$ is the standard deviation, and $C(\mathbf{x})$ is the (deterministic) estimated cost of that particular combinations of conservation investments (economic inputs into aquatic ecosystem service production) in the watershed.

The solution vector $\mathbf{x}^*$ defines the Pareto-efficient set (P_f), where each element is represented by a unique combination of cost, expected nutrient load and the standard deviation of loads:

$$P_f(\mathbf{x}^*) = \left\{C(\mathbf{x}^*), E_T[N(\mathbf{x}^*)]\,, Var[N(\mathbf{x}^*)]^{0.5} \;\middle|\nexists\, \mathbf{x} \neq \mathbf{x}^*, P_f(\mathbf{x}) \succ P_f(\mathbf{x}^*)\right\} \quad (2)$$

That is, a pattern of conservation investments defines the Pareto-efficient frontier if there is no other conservation action pattern which is a Pareto-improvement ($\succ$) in the cost-mean-standard deviation space. The Pareto-efficient frontier defines the set of optimal tradeoffs; for example, the lower envelope of the set with respect to mean N and conservation action costs gives the equivalent of the total abatement cost curve for expected nutrient pollution. It also offers valuable information on the possible mean-variance tradeoffs, where, for a given cost, a tradeoff between expected ecosystem service performance and its standard deviation could be seen. However, we cannot directly infer how much would it cost to achieve a particular level of nitrogen loads under different levels of resilience, where by resilience, we understand the probability of achieving that target in any given year. However, for the single stochastic objective, it is straightforward to "collapse" the three-dimensional Pareto-frontier into a set of

"resilient tradeoffs" between cost and resilient provision of an ecosystem service. Doing so involves appropriately constructing the deterministic equivalent to the resilience objective using the mean, standard deviation, and the critical value of the controlled distribution of the stochastic objective.

Finding resilient solutions involves solving a chance- constrained optimization problem:

$$Min_{\mathbf{x}}\ C(\mathbf{x})\ \ s.t.\ \ \Pr\{\mathrm{N_t}(\mathbf{x}) \leq \overline{N}\} \geq \alpha \quad \forall t = 1, \dots, T \tag{3}$$

where $\overline{N}$ is the target level of N loads, and α the desired level of resilience measured as the probability of achieving the target.

We use the Pareto-frontier $P_f(\mathbf{x}^*)$ and employ two approaches to approximate solutions to the above problem, approaches that we identify as "normal" and "non-parametric". Under both approaches, we transform equation (3) using its deterministic counterpart as:

$$Min_{\mathbf{x}}\ C(\mathbf{x})\ s.t.\ \ E_T\{\mathrm{N}(\mathbf{x})\} + \phi^{\alpha} Var(N(\mathbf{x}))_T^{0.5} \leq\ \overline{N} \tag{4}$$

where ϕ^{α} is the critical value of the standardized distribution of $N(\mathbf{x})$.

Note that a solution to the chance-constrained problem (3) must be a member of the Pareto frontier in the cost-mean-standard deviation space: $\hat{\mathbf{x}} \subset \mathbf{x}^*$. The converse is not true: that is, a particular solution from a multiobjective optimization program need not be optimal for a chance-constraint program. Appendix 1 in supplemental materials provides the demonstration of this point.

Under the normal approach, we assume the standardized distribution of pollution load follows a normal distribution and use $\phi^{\alpha} = \Phi^{-1}(\alpha)$, the standard normal critical value that depends on α (1.64 for $\alpha = 0.95$). Under the normality assumption, we consider $\alpha - resilient$ pollution loads to be $E_T\{\mathrm{N}(\hat{\mathbf{x}})\} + \Phi^{-1}(\alpha) Var(N(\hat{\mathbf{x}}))_T^{0.5}$ and can focus on the results in terms of tradeoffs between cost and resilient nitrogen loads.

Non-parametric approach

An alternative approach is to employ non-parametric bootstrap methods (Efron (1979)), and define the resilience pollution loads in terms of the bootstrapped quantiles. Since our data (nitrogen loads simulated over a period of time) is serially dependent, we employ the block stationary bootstrap method (Politis and Romano (1992), (1994)). Under this approach, observations are re-sampled in blocks of random length, with the length of the block being determined by a geometric distribution. The block re-sampling (observations are drawn consecutively) preserves the lag dependence in the original data. The bootstrapped data is stationary if the block length is determined using a geometric distribution. Additionally, the block bootstrap works well under very weak conditions on the dependency structure of the original data.

For any efficient combination of conservation practices ($\mathbf{x}^*$) that is part of the Pareto frontier $P_f(\mathbf{x}^*)$, we take the model-simulated $T \times 1$ vector of nitrogen values $N(\mathbf{x}^*)$ to construct a non-parametric distribution using a stationary bootstrapping approach using blocks of unequal length. To obtain tradeoffs involving $\alpha - resilient$ nitrogen loads, we compute, for each bootstrap replicate series, the sample α-quantile and average the results over many bootstrap replications. The interpretation of the new $\alpha - resilient$ Pareto frontier is similar to the previous one, each solution representing a non-dominated combination of cost and $\alpha - resilient$ nitrogen loads that correspond to a given level of resilience, α. The magnitude of the differences between the normal and non-parametric approaches is an empirical question.

Multiple pollutants: A case of nitrogen and phosphorus

We also consider developing tradeoffs which involve the means and the variances of multiple ecological objectives. In this case, we modify the multiobjective minimization problem

to include the means and standard deviations of two nutrient pollutants, nitrogen and phosphorus:[9]

$$Min_{\mathbf{x}}\,[\,C(\mathbf{x}),\ E_T[N(\mathbf{x})]\,, Var[N(\mathbf{x})]^{0.5}, E_T[P(\mathbf{x})]\,, Var[P(\mathbf{x})]^{0.5}] \quad (5)$$

where $\mathbf{x}$ represents a particular placement of conservation practices, $N(\mathbf{x})$, $P(\mathbf{x})$, the vectors of nitrogen and phosphorus loads of length T, $E[.]$ is the expected water quality outcome measured as (historical) sample mean of nitrogen and phosphorus, $Var[N(\mathbf{x})]^{0.5}$ and $Var[P(\mathbf{x})]^{0.5}$ are respective standard deviations, and $C(\mathbf{x})$is the estimated annual cost of the particular combination of conservation investments in the watershed.

Similarly to the univariate case, the solution is represented by a Pareto set, P_f^{NP}, where each element represent a non-dominant combination of cost, mean and standard deviation values for nitrogen and phosphorus emissions associated with a spatial combination of conservation practices. As discussed above, it is more intuitive to consider actual tradeoffs between mean and variance control or to characterize a particular solution in terms of a probability (resilience value) of meeting a specified target.

In order to characterize joint resilience implied by the solutions in the Pareto-frontier, we rely on the nonparametric bootstrap, now using two dimensions. Resilience is defined as the joint simulated probability of achieving both N and P targets. Similarly to the univariate stationary bootstrapping, we use the vectors of simulated nitrogen and phosphorus loads to generate bootstrap replicates using blocks of unequal length. The stationary bootstrapping procedure involves using both vectors simultaneously, thus preserving the correlation between controlled loads of N and P. That is, given a particular joint target $(\bar{N}, \bar{P})$, we can construct characterize the

[9] If the objective were to be specified as minimizing the variance, for example, the sum, or a linear index of two nutrients, the covariance term would enter into problem specification. Alternatively, the resilience objective specified as a joint probability could be simulated within the optimization loop (as in Poojari and Varghese (2008)). We leave those extensions to future work.

tradeoff frontier in terms of cost, mean nitrogen, mean phosphorus and simulated joint resilience of achieving the specified target. The resilience level is estimated as the simulated probability, $p(\mathbf{x}_i)$:

$$p(\mathbf{x}_i) = \sum_{r=1}^{M}\{\sum_{t=1}^{T} I(N(\mathbf{x})_{rt} \leq \bar{N}, P(\mathbf{x})_{rt} \leq \bar{P})/T\}/M \quad (6)$$

where T is the length of the model simulation, $\mathbf{x}_i$ is the particular pattern of conservation investments evaluated and M is the number of bootstrap repetitions.

To approximate the solution sets for the multiobjective problems (1) and (5), we use a simulation-optimization framework using Soil and Water Assessment Tool (SWAT) as the simulation model and a modification of the Strength Pareto Evolutionary Algorithm 2 (SPEA2) (Zitzler, Laumans, and Thiele, 2002) as the multiobjective optimization heuristic, as described by Rabotyagov et al. (2010). The simulation-optimization framework simultaneously minimizes the cost, the 20-year means ($T = 20$) and standard deviations of annual N for the single pollutant case and N and P loads for the two pollutant case.[10] The solutions are sets of Pareto-nondominated watershed configurations P_f and P_f^{NP}. To assess convergence, we use a consolidation ratio proposed by Goel and Stander (2010) and used by Rabotyagov et al. (2014).

SWAT is designed to run watershed simulations based on a wide range of inputs: weather data, soil characteristic, plant growth and crop rotations, nutrient management, nutrient transport and transformation, land use and management practices. The model can be used to estimate the changes in nutrient emission in response to the land changes associated with alternative conservation practice, crop choices, and rotation alternatives. The model was developed by the

[10] The resulting relatively small sample size used to construct the model-simulated mean and the standard deviation is one of the limitations of the study, and can introduce imprecision in resilience estimates. To the extent that mean and standard deviation estimates are not biased, we try to improve precision by bootstrapping optimized series.

U.S Department of Agriculture and has been used in a wide range of applications (Arnold et al. (1998); Arnold and Fohrer (2005); and Gassman et al. (2008)).

Empirical Application: The Boone River Watershed

Our empirical results focus on The Boone River Watershed (BRW). The BRW is a typical agricultural watershed in central Iowa with more than 90% of its area dedicated to corn and soybean production. The watershed's tributaries offer habitat to the Topeka shiner, a federally listed endangered species, and to other fish and mussel species. Additionally, the watershed tributaries feed the Des Moines River, a major water source for the biggest metropolitan area in Iowa. The lower part of the watershed is used for recreation activities.

Given the extent of the agricultural activities, high levels of agriculture-contributed nitrogen, phosphorus and sediment loads contribute to the water quality impairments. A successful calibration for the current Boone River Watershed SWAT baseline was obtained by using monthly streamflow nutrient data and incorporating earlier calibration efforts (Gassman, (2008)).[11] The set of conservation practices selected for achieving the nutrient reduction includes working land practices: cover crop, no-till, the combination of cover crops and no-till, and land retirement. Typically, cover crops are grown during late fall and early spring. In the Midwest, where there are no markets for cover crops, cover crops are promoted for their direct environmental benefits (recycle nutrient and prevent nutrients leaching) and indirect economic benefits (improve soil health by preventing soil erosion). Cover crops are effective in reducing both nitrogen and phosphorus losses. No-till is a type of tillage where no more than 30% of the

[11] The present SWAT simulations are being performed with an updated SWAT version 2012 code (SWAT2012, Release 6150 that contains corrected algorithms that more correctly simulate movement of nitrate through subsurface tile lines as well as numerous other enhancements that were not present in the SWAT2005 code.

crop residue is removed. No-till is effective in reducing erosion and phosphorus runoff. Land retirement involves taking land out of production and the establishment of perennial grasses.

The costs estimates for conservation practices used in this study are drawn from several sources: no-till at $6 per acre (Iowa State Extension budgets), cover crops at $35 per acre (Iowa Nutrient Reduction Strategy), $41 per acre for the combination of no-till and cover crops, and $254 per acre, the average cash rental rate for the BRW (Iowa State Extension cash rental rates estimates) as the cost of land retirement. The cost of conservation practices is additional to the cost of baseline activities, considered to be zero in this application.

Results and discussion

The simulation framework allows us to evaluate counterfactual watershed-based scenarios in terms of estimated costs of conservation practices and their implications for mean and variance of corresponding nutrient loads over a 20-year period (1993-2013). We estimate the Pareto- efficient frontiers for a single pollutant (N) and multiple pollutants (N and P). We offer a short analysis of the mean-variance tradeoffs and how these tradeoffs relate to the choice of the conservation actions. Next, we analyze the trade-offs between achieving a pollution target with a given resilience level and the estimated cost of conservation actions. The set of resilience values (α) ranges from 50 percent to 95 percent in increments of 5 percent, as well as 99 percent. Nutrient pollution targets are chosen to be equivalent to a range of percent reductions from the historical baseline emissions.

Single pollutant case: Nitrogen, Mean-Variance Tradeoffs

The results of the multi-objective optimization defined by equation (1) can be visually depicted by a three dimensional scatterplot (P_f), where each point on the frontier represents the least cost watershed configuration that achieves a given expected value of N loads and has the lowest standard deviation (see Figure A2 in the supplementary material). Figure 1 depicts the extent of

the mean-variance tradeoffs from the frontier. Specifically 1(a) shows a fairly linear positive relationship between the mean and the standard deviation of N loads, as standard deviations increase with the means. Additionally, the analysis of mean-coefficient of variation (ratio of standard deviation to the mean) plot (Figure 1(b)) shows three patterns: a steep increasing trend for the low range nitrogen emissions (below three thousand tons) where the standard deviation increases at a faster rate than the mean, followed by a smoother declining pattern where the standard deviation increases at a slower rate than the mean. For larger loads (above 4.5 thousand tons), the ratio of standard deviation to mean settles around 0.5. These patterns can be explained by the distribution of the conservation practices selected by the algorithm (see supplementary material Figure A3).

Next, we quantify the cost to achieve a particular level of nitrogen loads under different levels of resilience. More explicitly, for any level of resilience α, we construct resilient Pareto frontiers, where each Pareto frontier can be viewed as the total cost curve where the corresponding nitrogen emissions are achieved with probability α. As previously described, we use two approaches (normal and non-parametric) to construct the resilient Pareto frontiers that corresponds to different resilience levels. The "normal" approach assumes that the standard normal critical values are used to weigh the standard deviations, while the non-parametric approach uses stationary bootstrap to simulate the quantiles. Simulated nutrient load series pass stationarity tests, and we use 10,000 bootstrap replications with mean block length of 5. The new Pareto frontiers transform the mean nitrogen values of the original Pareto frontier into α resilient levels while keeping the costs and the watershed configurations unchanged.

Figures 2 depicts the α resilient Pareto frontiers for four levels of resilience: median (50), 75, 90, and 99 given the two approaches, as well as the mean-cost tradeoff. The horizontal axis depicts the resilient loads, and the vertical axis shows annual costs. Notice that under the normal

approach (left panel), the corresponding levels of resilience for mean and median are identical, while under the non-parametric approach the two tradeoff frontiers are different, the bootstrapped mean curve being entirely above the median (right panel). Under the both approaches, the Pareto frontiers move further away from the left corner as the resilience levels increase. For any cost level (consider a horizontal line), the resilient level of N loads increases as we move from one frontier to another. This shows us how much resilience can be achieved under a given budget. Likewise, for any level of resilient N loads, the cost increases as we move from one frontier to another. The distance between two consecutive frontiers represents how much it would cost to make the same level of N load more resilient. (Pairwise comparisons between the two distributions are provided in the supplementary material).

Each cost-resilient curve corresponds to a resilient N target expressed as a percentage reduction from the baseline. As expected, more stringent targets (higher percentage reductions, lower loads) cost more and the costs of achieving a given target increases with the resilience level. For less stringent targets, the costs-resilience curves are convex, with a non-convexity patterns for more stringent targets. For example, when the target is set to 70 percent reductions, the cost is flat once a high level of resilience (80) is achieved.

Resilience-Marginal Cost Curves

Another way to analyze the resilience-cost trade-off is to answer the question how much would it cost to achieve an additional level of resilience. We focus our analysis on three levels of reductions: low (20 percent), average (the Iowa Nutrient Reduction Strategy 45 percent), and high (70 percent reductions). For each of the three targets, Figure 3 summarizes the cost curves for securing the targets at an additional resilience level. These curves can be interpreted as the marginal cost of resilience. Although the marginal cost curves have a similar shape, their magnitudes differ across the two approaches. The marginal cost curve when the target is low (20

percent reductions) is almost flat for resilience levels lower than 80. However, for higher resilience, the marginal costs display a sharp increase, with the increase being sharper under normal approach. The marginal cost curve for the intermediate target displays more than one pattern. Under the normal approach, marginal costs are increasing for lower resilience, linear for moderate resilience, and again increasing for higher resilience levels. However, the patterns are different under the non-parametric approach: linear for lower levels, increasing for moderate levels, decreasing and linear for higher levels of resilience. The marginal costs for the most stringent target are increasing for lower levels, decreasing for moderate levels, and linear for higher resilience level. The diversity of patterns across targets and resilience levels can be explained by the distribution of the conservation practices (these are provided in Table A1 of supplementary materials). The costs of achieving resilient loads corresponding to 45 percent reductions (3.39 thousand tons) range from 13 to 87 million over the considered resilience levels. Similarly to McSweeny and Shortle (1990), we find that to control a single-year N load with 99 percent resilience is almost 7 times costlier than controlling N with median resilience

Resilient N loads for different cost (budget) levels

The α resilient Pareto frontiers can also provide insight into the different load levels that can be secured under different levels of resilience when we impose a limit on total costs (iso-cost curves). Figure 4 can be used to see how much resilience can be obtained under a given budget. Next, we present the results for four cost (budget) levels: 10, 20, 50, and 100 million. For each budget level, we construct iso-cost curves showing the tradeoffs between resilience and different levels of attainable loads.

Figure 4 shows that the iso-costs are convex shaped, showing that when considering cost constant, higher levels of resilience translate in higher levels of emissions, or alternatively lower emission level have lower resilience levels. The empirical findings also show that the size of

these tradeoffs decrease as the total costs increase, as the iso-cost curves corresponding to lower total cost have steeper slopes. For any of the chosen cost and any resilience levels, fewer emissions (more reductions) can be claimed under the non-parametric approach (Figure 4 right vs. left panel). Also, the slopes of the non-parametric iso-cost curves are smoother.

Multiple targets: nitrogen and phosphorus

Next, we present the simulation results for the case when two pollutants (N and P) are jointly targeted. We approximate the Pareto-frontier for 5 objectives: cost and means and standard deviations of N and P. Pareto-frontier we obtain is valuable in that can show the nature of tradeoffs along different values of N and P as well as corresponding variability and cost.

Visualizing tradeoffs across more than two dimensions is challenging, and pairwise projections of the Pareto-frontier could be most helpful to see a particular scope of synergies or tradeoffs. Visualizing across 5 dimensions is possible; however, interpretation can be challenging. To aid this process, we present a radar (spider) plot in all 5 dimensions. Specific solutions of interest (a few at a time) can be analyzed as well. Consider the left panel of Figure 5, and the mean N (mean P) and Cost axes. The non-convex shape of the plot between those axes says that there are no solutions in the Pareto-frontier which simultaneously have high cost and high mean N (and P) loads (and compensating for those with smaller values on other axes). This suggests a strong tradeoff existing between mean nutrient loads and cost. A convex shape with respect to other axes *does not* mean that tradeoffs do not exist among the remaining pairs of objectives, but that there *exist* efficient solutions which exhibit synergies (co-movement) along those dimensions. For example, as we see subsequently (Figure 6), tradeoffs between N and P control exist, but synergies are also present (pairwise comparison of mean N and P on the right panel of figure 5). A presence of at least some synergies is also apparent by considering pairwise tradeoffs between means and standard deviations (consistent with a limited nature of mean-

variance tradeoff for N explored above). Whereas, as can be seen from the nature of the tradeoffs between costs and standard deviations (shown on the right panel of Figure 5 for the case of standard deviation of P—N results are similar), there are no synergies between cost and risk, and we see strong tradeoffs consistent with the notion that resilience is always costly. However, we do not see strong tradeoffs between means or standard deviations of nutrient reduction objectives. Of course, this finding may not generalize to other contexts.

Next, we make the connection to resilience. Note that, unlike in a single stochastic objective case, we can no longer claim that a solution to a chance-constrained formulation has to be a member of the Pareto-frontier. For the case of separate resilience objectives, where each pollutant has be controlled in a resilient fashion that is still the case (using the same logic as above). That is, single pollutant resilient levels can be obtained in exactly the same way we proceeded above with N. Because of that reason, we do not present single-pollutant resilience tradeoffs.

However, if one is interested in the joint constraint of the type: $\Pr\{\mathrm{N_t}(\mathbf{x}) \leq \overline{N}, P_t(\mathbf{x}) \leq \overline{P}\} \geq \alpha \quad \forall t = 1, \dots, T$, we cannot be assured of joint resilience optimality of solutions obtained by the multiobjective program, as the algorithm does not directly simulate joint probability which is a function of variances and the covariance between N and P. To assume cost-joint resilience efficiency for specific $\overline{N}$ and $\overline{P}$ targets, one could formulate a two-objective evolutionary optimization program involving cost and simulated probability of joint goal attainment (akin to Poojari and Varghese (2008) or Rabotyagov, Jha, and Campbell (2010)). Despite the possibility that the solutions in the Pareto frontier may not be optimally resilient for joint nutrient targets, we can still provide ex-post assessment of the solutions in terms of joint resilience. To do so, we again rely on (now joint) non-parametric bootstrap approach, using 10,000 replicates and computing the simulated resilience using (6).

A three dimension illustration of these tradeoffs when the targets are set equal to 45 percent reductions for both N and P (equation 9) is presented in the supplemental material (Figure A6). Each element on this frontier (a 3-dimensional projection of the 5-dimensional Pareto-frontier P_f^{NP}) is assessed for a resilience (probability) level of achieving this joint target. As for the single pollutant case: securing higher level of resilience demands higher costs. We present the lower envelopes of the plot in Figure 6. Figure 7 depicts the marginal costs of achieving additional levels of resilience for the three specified targets, while Table A2 (contained in supplementary details) describes in detail the total and marginal costs as well as the distribution of conservation practices. For example, the least cost way to achieve 45 percent reductions with 70 percent resilience is higher than the least cost to achieve the same level of reductions with 75 percent resilience (Figure 6). The negative marginal costs are unexpected but we interpret them as the inefficiencies embedded in the spikes, and, should one focus on a specific set of N and P reductions with a resilience objective, we expect those to disappear. With those caveats in mind, we provide a broad assessment of joint resilience implied by the 5-dimensional Pareto-frontier.

Overall, the costs of achieving the joint target are higher than in the case of a single pollutant and range from 22.3 to 107.4 million. This is to be expected as a joint probability is going to be smaller than a marginal one. The distribution of the conservation practice is different, with more land retirement being used more extensively at any resilience level. The spatial placement of the conservation practices associated with these solutions is provided in the supplemental materials.

Conclusions and caveats

Many ecosystem services are rival and important tradeoffs exist in their production process. Understanding the nature of these tradeoffs requires: *(a)*defining a quantifiable measure

of the underlying ecosystem production process and of the economic inputs that go into this productions functions, and *(b)* exploring alternative resource allocation decisions to identify, if only approximately, Pareto-efficient ways of producing different ecosystem services. Uncertainty in the provision of a particular ecosystem service adds another dimension to the nature of these tradeoffs, where different ecosystem services differ both in terms of the expected outcomes and in terms of risks. Closely related to uncertainty is the notion of resilience, and the cost of providing the ecosystem service under different levels of desired resilience.

We focus on understanding and quantifying the tradeoffs for the case of proxies for aquatic ecosystem services in the landscapes dominated by agricultural activity. Particularly, we focus on controlling the flux of agricultural nutrients (N and P) as means to improve the upstream and downstream water quality. Economic inputs into water quality production are a set of conservation practices that can be implemented on agricultural landscapes for controlling the flux of nutrients, while the (intermediate) ecological production function is an ecohydrologic simulation model relating human actions to changes in nutrient loads. By integrating a heuristic global optimization with a ecohydrologic model we meet the conditions of having science-based representation of the water quality production function ($W_t(\mathbf{r}(\mathbf{x}, \boldsymbol{\xi}_t))$) and its dependence on the exogenous stochastic weather factors and of having the ability to produce an approximate Pareto-frontier that accounts for multiple tradeoff dimensions.

We quantify the tradeoffs involved in achieving different levels of nutrient loads with different levels of resilience where resilience is defined as the probability of attaining the desired level of nutrient load. We spatially optimize the selection of least-cost patterns of agricultural conservation practices or both the expected performance of the conservation actions and its variance. We analyze the tradeoffs for a single nutrient (ecosystem service), and then expand our analysis to include multiple nutrients (multiple ecosystem services).

We apply our modeling framework to the Boone River Watershed in Iowa. The empirical results confirm expectations and are consistent with previous studies: securing nutrient loads with higher level of resilience is costly. However, the marginal cost is not necessarily increasing: that is, focusing on larger nutrient reductions allows one to obtain resilience at a smaller additional cost than if one is seeking only modest nutrient reductions. In our application, this is due to the ability of perennial grassland to buffer against exogenous shocks and to drastically reduce variability in nutrient loads (as shown before, e.g., in Rabotyagov, Jha, and Campbell 2010). Furthermore, the main tradeoff dimension is between cost of conservation investments and ecosystem service objectives, as opposed to pronounced mean-variance tradeoffs or strong tradeoffs between the two nutrient objectives. While some meaningful tradeoffs exist between nutrient objectives, our findings highlight the presence of relative synergies in agricultural conservation investments aimed at nutrient reductions. However, while *relative* synergies exist, controlling risk of nutrient loads has high opportunity costs, and resilience comes at a significant premium.[12]

Among many caveats, we point out that our optimization algorithm was not exactly tailored to the optimal joint resilience question, but instead focused on providing an overall picture of feasible tradeoffs. Additional limitations associated with uncertainty in model structure, the simplicity of economic cost representation, and the level of spatial resolution of the ecohydrologic model present ample opportunities for future research. However, we hope to show the utility and the promise of the general approach which integrates scientific understanding of

[12] We note recent research by Carpenter et al. (2015) who provide examples where, in nonlinear systems, reducing high-frequency variance can lead to an increase in low-frequency variance, thereby undermining the resilience objective. We constructed spectrum plots of controlled variance of nutrients and we see a decrease in variance at all spectra with an increase in conservation investment cost.

complex systems with the practical need to see how production of non-market ecosystem services can be accomplished at the lowest possible sacrifice of economic inputs.

1

Longer Abstract

Many ecosystem services are rival and important tradeoffs exist in their production process, while some jointness in production (synergies) are also postulated to exist. We assess the strength of tradeoffs and synergies involved in reducing agriculture-generated watershed nutrient loads with different levels of resilience. We define resilience as the simulated probability of attaining the desired level of nutrient load. We spatially optimize the selection of least-cost patterns of agricultural conservation practices or both the expected performance of the conservation actions and its variance. The modeling framework is applied to the Boone River Watershed in Iowa. The empirical results confirm that securing nutrient loads with a higher level of resilience is costly. However, the marginal cost is not necessarily increasing: focusing on larger nutrient reductions allows one to obtain resilience at a smaller additional cost than if one is seeking only modest nutrient reductions. In our model, this is due to the ability of perennial grassland to buffer against exogenous shocks and to drastically reduce variability in nutrient loads. In extending the model to two nutrients, nitrogen and phosphorus, we find that the main tradeoff dimension is between cost of conservation investments and ecosystem service objectives, as opposed to pronounced mean-variance tradeoffs or strong tradeoffs between the two nutrient objectives. While some meaningful tradeoffs exist between nutrient objectives, our findings highlight the presence of relative synergies in agricultural conservation investments aimed at nutrient reductions. However, while *relative* synergies exist, controlling risk of nutrient loads is once again shown to have high opportunity costs, and resilience comes at a significant premium.

Figure 1 (a) Mean-Variance Trade-Offs (b) Mean-Coefficient of Variation

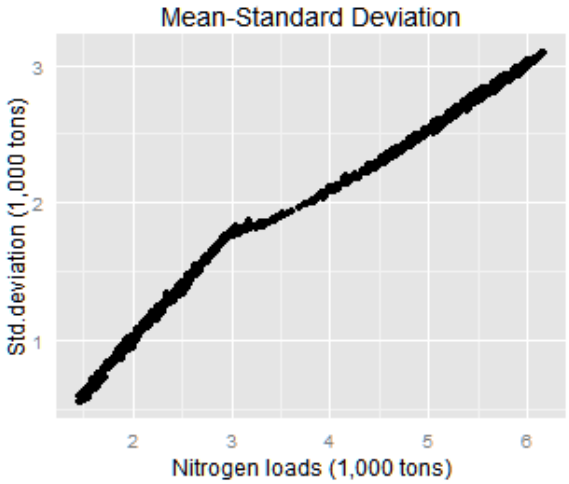

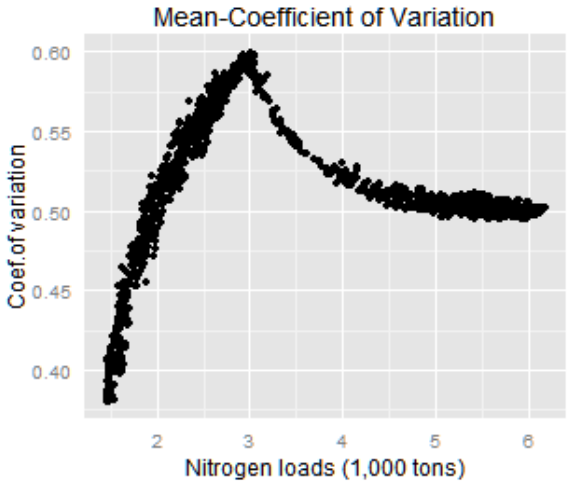

Figure 2: α Resilient Pareto Frontiers (Normal Approach (left), Non-parametric Approach (right))

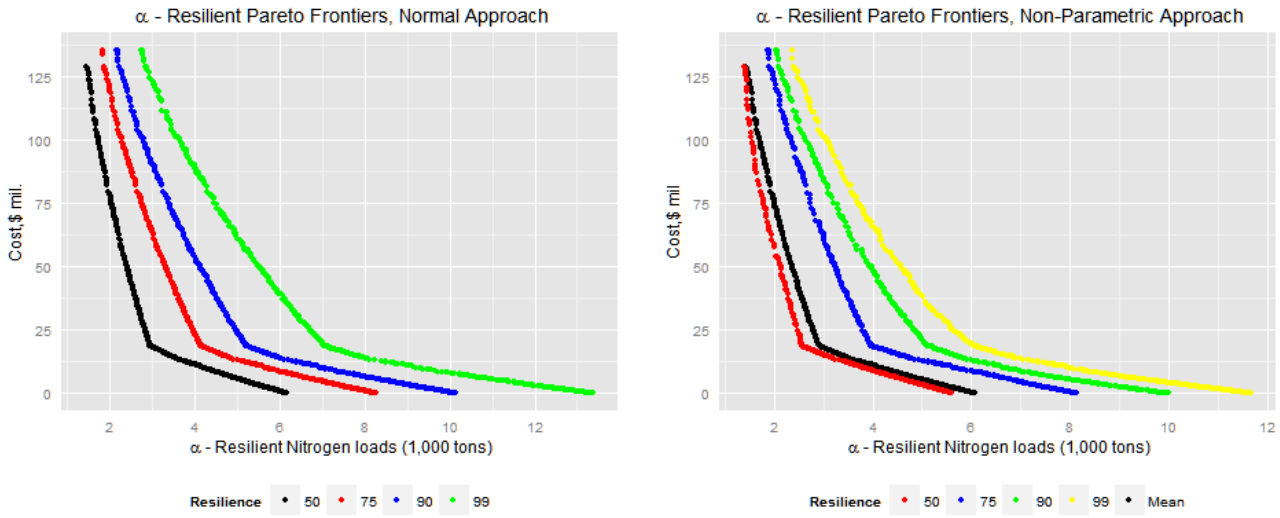

Figure 3 Marginal Costs of Additional Resilience for Different Resilient N Targets

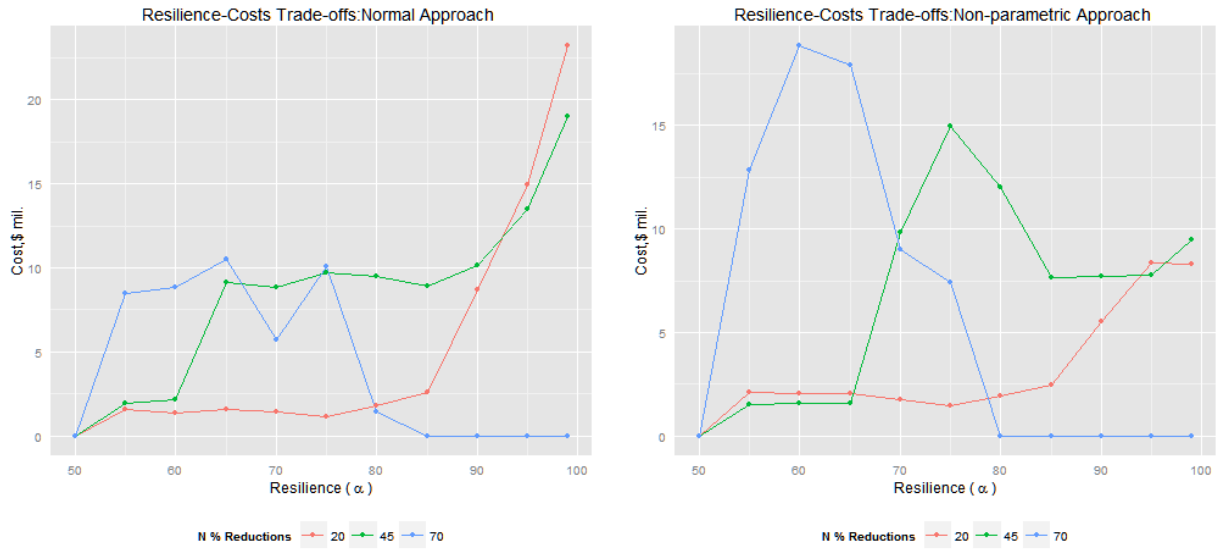

2

Figure 4 Resilience: Iso-Cost Curves(Normal Approach: left, Non parametric approach right)

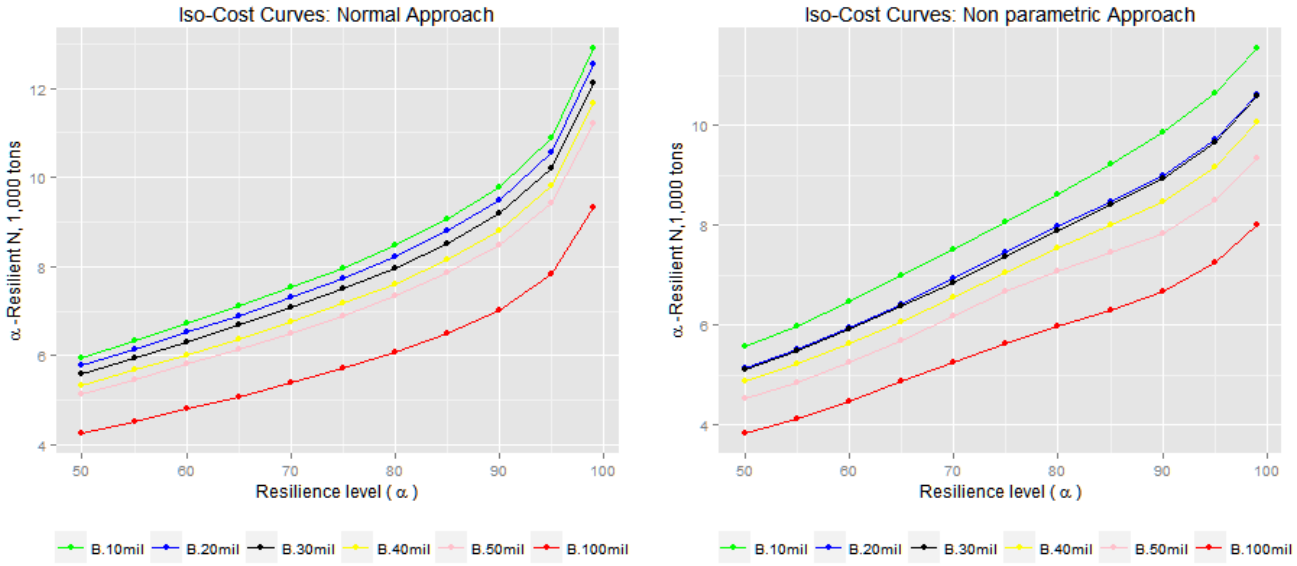

Figure 5. Pareto Optimal Frontier: Cost, Means (N, P), Standard deviation (N ,P)

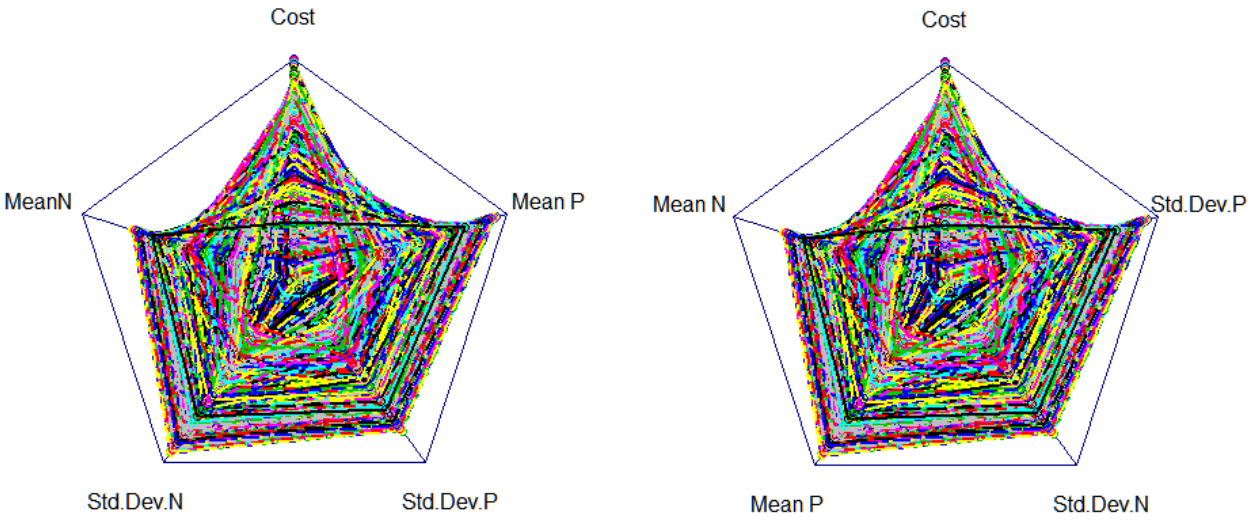

Figure 6 Cost of Achieving Resilience When Target is Equal to 45 percent Reductions for Both N and P.

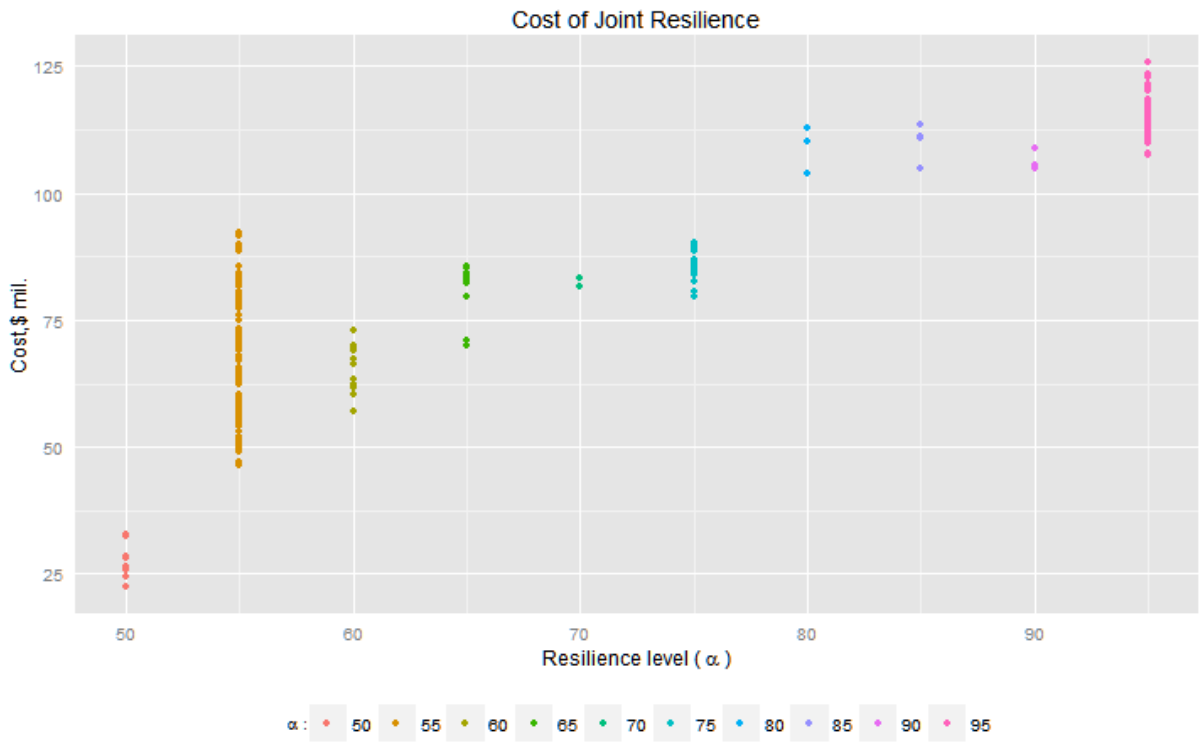

Figure 7 Marginal Costs of Joint Resilience

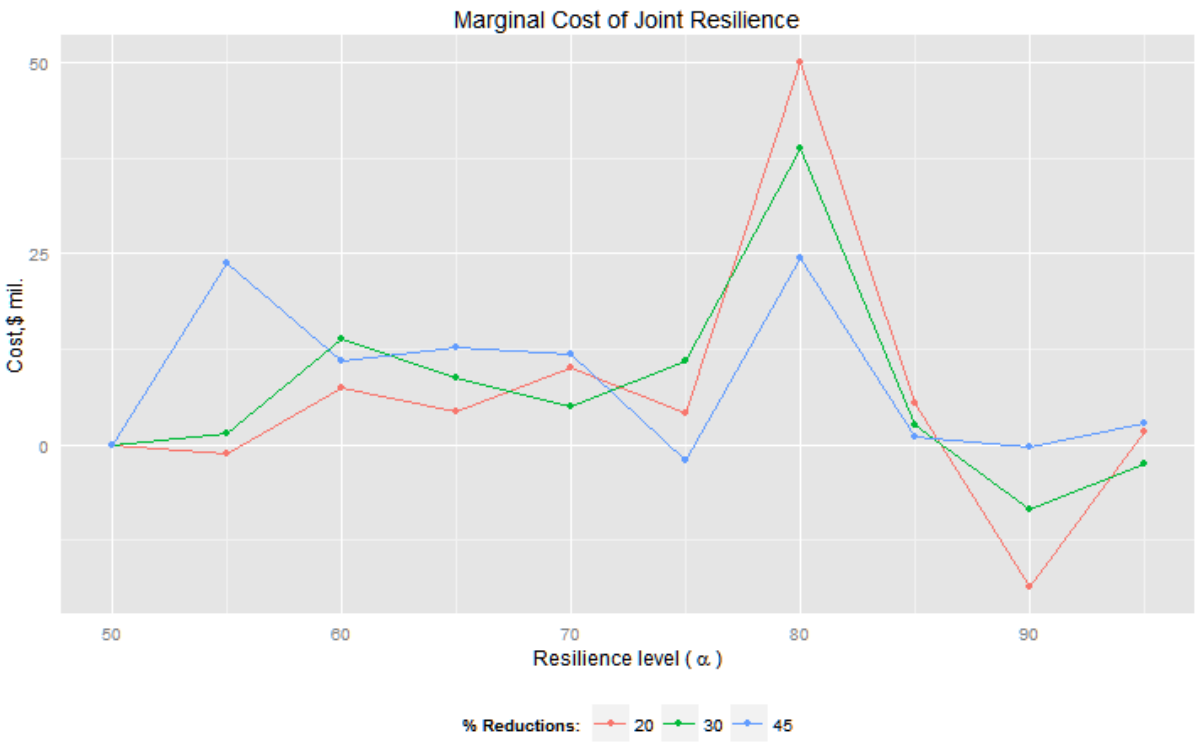
Marginal Cost of Joint Resilience
50
25
0
Cost,$ mil.
50
60
70
80
90
Resilience level (α)
% Reductions:
20
30
45

References

Ahmadi, M., Arabi, M., Hoag, D. L., & Engel, B. A. 2013. A Mixed Discrete-Continuous Variable Multiobjective Genetic Algorithm for Targeted Implementation of Nonpoint Source Pollution Control Practices. *Water Resources Research* 49(12): 8344-8356.

Arnold,J.G.,R.Srinivasan, R.S., Muttiah, and J.R.Williams.1998.Largeareahydrologic modeling and assessment part I: model development. *Journal of the American Water Resources Association* 34(1): 73–89.

Arnold, J. G. and N. Fohrer. 2005. SWAT2000: current capabilities and research opportunities in applied watershed modelling. *Hydrological processes*, *19*(3), 563-572.

Barbier, E. B., Koch, E. W., Silliman, B. R., Hacker, S. D., Wolanski, E., Primavera, J., ... & Reed, D. J. 2008. Coastal Ecosystem-Based Management with Nonlinear Ecological Functions and Values. S*cience* 319(861): 321-323.

Bateman, I., A. R. Harwood, G. M. Mace, R.T. Watson, D.J. Abson, B.Andrews, A. Binner et al. 2013."Bringing Ecosystem Services into Economic Decision-making: Land Use in the United Kingdom." *Science* 341(6141): 45-50.

Bawa, V. S. 1973. On Chance Constrained Programming Problems with Joint Constraints. *Management Science 19*(11): 1326-1331.

Beavis, B., and M. Walker. 1983. Achieving Environmental Standards with Stochastic Discharges. *Journal of Environmental Economics and Management 10*(2):103-111.

Bigman, D. 1996. Safety-first Criteria and their Measures of Risk. *American Journal of Agricultural Economics 78*(1): 225-235.

Bostian, M., G. Whittaker, B. Barnhart, R. Färe, and S. Grosskopf. 2015. Valuing Water Quality Tradeoffs at Different Spatial Scales: An Integrated Approach using Bilevel Optimization. *Water Resources and Economics* 11:1-12.

Boyd J., and S. Banzhaf. 2007. What are Ecosystem Services? The Need for Standardized Environmental Accounting Units. *Ecological Economics* 63(2-3):616–626.

Byström, O., H. Andersson, and M. Gren. 2000. Economic Criteria for using Wetlands as Nitrogen Sinks under Uncertainty. *Ecological Economics*, *35*(1): 35-45.

Carpenter, S., R., Brock, W. A., Folke, C., van Nes, E. H., and M. Scheffer. 2015. Allowing Variance May Enlarge the Safe Operating Space for Exploited Ecosystems. *Proceedings of the National Academy of Sciences* (11): 800-804.

Charnes, A., and W.W. Cooper, W. W.1959. Chance-constrained programming. *Management science*, *6*(1), 73-79.

Cherubini, U., E. Luciano, and W.Vecchiato. 2004. *Copula Methods in Finance*. John Wiley & Sons.

Chichakly, K. J., W.B. Bowden, and M.J. Eppstein. 2013. Minimization of Cost, Sediment Load, and Sensitivity to Climate Change in a Watershed Management Application. *Environmental Modelling & Software* (50):158-168.

Deb, K. 2001. Multi-objective optimization using evolutionary algorithms (Vol. 16). John Wiley & Sons.

Elofsson, K. 2003. Cost-effective Reductions of Stochastic Agricultural Loads to the Baltic Sea. *Ecological Economics*, 47(1):13-31.

Efron, B. 1979. Bootstrap methods: another look at the jackknife. *The annals of Statistics*, 1-26.

Evans-White, M. A., B.E. Haggard, and J.T. Scott. 2013. A Review of Stream Nutrient Criteria Development in the United States. *Journal of Environmental Quality*, *42*(4):1002-1014.

Gramig, B. M., C. J. Reeling, R. Cibin, and I. Chaubey. 2013. Environmental and Economic Trade-offs in a Watershed when Using Corn Stover for Bioenergy. *Environmental Science & Technology*, *47*(4): 1784-1791.

Gren, M. 2010. Resilience Value of Constructed Coastal Wetlands for Combating Eutrophication. *Ocean & Coastal Management*, *53*(7): 358-365.

Gren, M. 2008. Adaptation and Mitigation Strategies for Controlling Stochastic Water Pollution: An Application to the Baltic Sea. *Ecological Economics 66*(2): 337-347.

Gren, M., G. Destouni, and R. Tempone. 2002. Cost Effective Policies for Alternative Distributions of Stochastic Water Pollution. *Journal of Environmental Management*, *66*(2): 145-157.Gassman, P. W. 2008. *A simulation assessment of the Boone River watershed: Baseline calibration/validation results and issues, and future research needs*. ProQuest

Goel, T. and N. Stander .2010. A non-dominance-based online stopping criterion for multi-objective evolutionary algorithms. *International Journal for Numerical Methods in Engineering*, *84*(6), 661-684.

Heal, G., G. C. Daily,P.R.Ehrlich, J.Salzman, C.Boggs, J.Hellrnan,,and T. Ricketts. 2001 Protecting Natural Capital Through Ecosystem Service Districts. *Stanford Environmental Law Journal*, *20*, 333.

Heal, G. M. and A. A. Small. 2002. Agriculture and Ecosystem Services. *Handbook of Agricultural economics* (2):1341.

Herman, J. D., H.B. Zeff, P.M. Reed, and G.W. Characklis. 2014. Beyond Optimality: Multistakeholder Robustness Tradeoffs for Regional Water Portfolio Planning under Deep Uncertainty. *Water Resources Research 50*(10): 7692-7713.

Heiskary, S. A., R.W. Bouchard Jr. 2015. Development of Eutrophication Criteria for Minnesota Streams and Rivers using Multiple Lines of Evidence. *Freshwater Science*, *34*(2).

Hong, L. J., Y. Yang, and L. Zhang. 2011. Sequential Convex Approximations to Joint Chance Constrained Programs: A Monte Carlo Approach. *Operations Research 59*(3): 617-630.

Horan, R. D. and J.S. Shortle. 2011. Economic and Ecological Rules for Water Quality Trading. *JAWRA Journal of the American Water Resources Association*, *47*(1): 59-69.

Kampas, A. and B. White. 2003. Probabilistic Programming for Nitrate Pollution Control: Comparing Different Probabilistic Constraint Approximations. *European Journal of Operational Research*, *147*(1): 217-228.

Kampas, A. and K. Adamidis. 2005. Discussion of the paper "Cost Effective Policies for Alternative Distributions of Stochastic Water Pollution" by Gren, Destouni and Tempone. *Journal of Environmental Management*, *74*(4): 383-388.

Karp, D. S., C.D. Mendenhall, E. Callaway, L.O. Frishkoff, P.M. Kareiva, P. R. Ehrlich, and G.C. Daily. 2015. Confronting and Resolving Competing Values behind Conservation Objectives. *Proceedings of the National Academy of Sciences*, *112*(35): 11132-11137.

Kennedy, M. C., E.D. Ford, P. Singleton, M. Finney, and J.K. Agee. 2008. Informed Multi-Objective Decision-Making in Environmental Management using Pareto Optimality. *Journal of Applied Ecology 45*(1): 181-192.

Kling, C. L. 2011. Economic Incentives to Improve Water Quality in Agricultural Landscapes: Some New Variations on Old Ideas. *American Journal of Agricultural Economics*, *93*(2): 297-309

Kurkalova, L. A. 2005. Carbon Sequestration in Agricultural Soils: Discounting for ncertainty. *Canadian Journal of Agricultural Economics/Revue canadienne d'agroeconomie 53*(4): 375-384

Lankoski, J. and M. Ollikainen. 2003. Agri-environmental Externalities: A Framework for Designing Targeted Policies. *European Review of Agricultural Economics 30*(1):51-75.

Lichtenberg, E. 2002. Agriculture and the Environment. *Handbook of Agricultural Economics*, *2:* 1249-1313.

Lichtenberg, E. and D. Zilberman. 1988. Efficient Regulation of Environmental Health Risks. *The Quarterly Journal of Economics* (89): 167-178.

Longstaff, P. H., T.G. Koslowski, and W. Geoghegan. 2013. Translating Resilience: A Framework to Enhance Communication and Implementation. In *Symposium on Resilience Engineering* (pp. 12-23).

Maier, H. R., Z. Kapelan, J. Kasprzyk, J. Kollat, L.S. Matott, M. C. Cunha, and P.M. Reed. 2014. Evolutionary Algorithms and other Metaheuristics in Water Resources: Current Status, Research Challenges and Future Directions. *Environmental Modelling & Software*, *62*:271-299.

McSweeny, W. T. and J.S. Shortle. 1990. Probabilistic Cost Effectiveness in Agricultural Nonpoint Pollution Control. *Southern Journal of Agricultural Economics 22*(1): 95-104.

Mueller, N. D., E.E. Butler, K. A. McKinnon, A. Rhines, M. Tingley, N.M., Holbrook, and P. Huybers. 2015. Cooling of US Midwest Summer Temperature Extremes from Cropland Intensification. *Nature Climate Change*.

Muller, N. Z., R. Mendelsohn, and W. Nordhaus. 2011. Environmental Accounting for Pollution in the United States Economy. *The American Economic Review*, 1649-1675.

Nicklow, J., P. Reed, D. Savic, T. Dessalegne, L, Harrell, A. Chan-Hilton, M. Karamouz et al. "State of the art for genetic algorithms and beyond in water resources planning and management." *Journal of Water Resources Planning and Management* 136, no. 4 (2009): 412-432.

Paris, Q. 1979. Revenue and Cost Uncertainty, Generalized Mean-variance, and the linear complementarity problem. *American Journal of Agricultural Economics*, *61*(2), 268-275.

Parkhurst, G. M., and J.F. Shogren, J. F. 2007. Spatial Incentives to Coordinate Contiguous Habitat. *Ecological Economics*, *64*(2): 344-355.

Polasky, S. and K. Segerson. 2009. Integrating Ecology and Economics in the Study of Ecosystem Services: Some Lessons Learned. *Annual Review of Resource Economics* 1: 409-434.

Polasky, S., E. Nelson J. Camm, B. Csuti, P. Fackler, E. Lonsdorf, and C. Tobalske. 2008. Where to Put Things? Spatial Land Management to Sustain Biodiversity and Economic Returns *Biological Conservation 141*(6): 1505-1524.

Politis, D. N. and J.P. Romano. 1992. A circular block-resampling procedure for stationary data. *Exploring the limits of bootstrap*, 263-270.

Politis, D. N. and J.P. Romano.1994. The stationary bootstrap. *Journal of the American Statistical association*, *89*(428), 1303-1313.

Poojari, C. A., and Varghese, B. (2008). Genetic algorithm based technique for solving chance constrained problems. *European journal of operational research,185*(3), 1128-1154.

Porto, M. and O. Correia and P. Beja. 2014. Optimization of Landscape Services under Uncoordinated Management by Multiple Landowners.

Prekopa, A. 1970. On Probabilistic Constrained Programming. In *Proceedings of the Princeton Symposium on Mathematical Programming* (pp. 113-138). Princeton, NJ: Princeton University Press.

Proceedings of the National Academy of Sciences,

http://www.pnas.org/cgi/collection/nature_capital

Rabotyagov, S. S. (2010). Ecosystem Services under Benefit and Cost Uncertainty: An Application to Soil Carbon Sequestration. *Land Economics 86*(4): 668-686.

Rabotyagov, S. S., M. Jha, and T.D. Campbell. 2010. Nonpoint-Source Pollution Reduction for an Iowa Watershed: An Application of Evolutionary Algorithms. *Canadian Journal of Agricultural Economics/Revue canadienne d'agroeconomie*, *58*(4): 411-431.

Rabotyagov, S. S., T. D. Campbell, M. White, J.G. Arnold, J. Atwood, M. L.Norfleet, C.L. Kling et al. "Cost-effective targeting of conservation investments to reduce the northern Gulf of Mexico hypoxic zone." *Proceedings of the National Academy of Sciences* 111, no. 52 (2014): 18530-18535.

Roy, A. D. 1952. Safety First and the Holding of Assets. *Econometrica* 431-449.

Shortle, J. and R.D. Horan. 2013. Policy Instruments for Water Quality Protection. *Annu. Rev. Resour. Econ.*, *5*(1): 111-138

Steffen, W., K. Richardson, J. Rockström, S.E. Cornell, I. Fetzer, E.M. Bennett, and S. Sorlin. 2015. Planetary Boundaries: Guiding Human Development on a Changing Planet. *Science*, *347*(6223): 1259855.

Tóth, S. F. and M.E. McDill. 2009. Finding Efficient Harvest Schedules under Three Conflicting Objectives. *Forest Science* 55(2): 117-131.

USDA-CEAP, Wildlife National Assessment. 2015. http://www.nrcs.usda.gov/wps/portal/nrcs/detailfull/national/technical/nra/ceap/na/?cid=nrcs143_014151

US EPA, 2015 http://www2.epa.gov/nutrientpollutionWillis, D. B. and N.K. Whittlesey. 1998. The Effect of Stochastic Irrigation Demands and Surface Water Supplies on On-Farm Water Management. *Journal of Agricultural and Resource Economics* 206-224.

Zitzler, E., M. Laumanns, and L.Thiele.2002. "Spea2: Improving the strength pareto evolutionary algorithm for multiobjective optimization." *Evolutionary Methods for Design, Optimization, and Control* (2002): 95-100.

Appendix 1

As noted in the text, a solution to the chance-constrained problem (3) must be a member of the Pareto frontier in the cost-mean-standard deviation space: $\hat{\mathbf{x}} \subset \mathbf{x}^*$. The converse is not true: that is, a particular

solution from a multiobjective optimization program need not be optimal for a chance-constraint program. Obtaining a Pareto-frontier (and a mean-variance frontier) is, in principle, more general, and the specific weight placed on the standard deviation determines the point of "tangency" between the efficient frontier and the "α-isoresilient" pollution load line of form $E_T\{\mathrm{N}(\hat{\mathbf{x}})\} + \phi^{\alpha} Var(N(\hat{\mathbf{x}}))_T^{0.5} \equiv N(\alpha)$. Figure 1 graphically depicts this point. For a particular weight ϕ^{α} placed on the standard deviation, point A in the Pareto-frontier would be optimal, while point B would appear to be suboptimal given ϕ^{α}. However, for a different reliability requirement associated with a lower probability of reaching pollution reduction goal, point B would be optimal. These considerations require us to "post-process" the simulated Pareto-frontier when they are collapsed to "resilient" pollution quantities to eliminate original members of the mean-variance efficient frontiers which appear dominated given a specific distributional assumption or the desired level of resilience. By construction, any nitrogen load level equal to $N(\alpha)$ is achieved with probability α.

Figure A1: Pareto frontier and mean-variance minimums

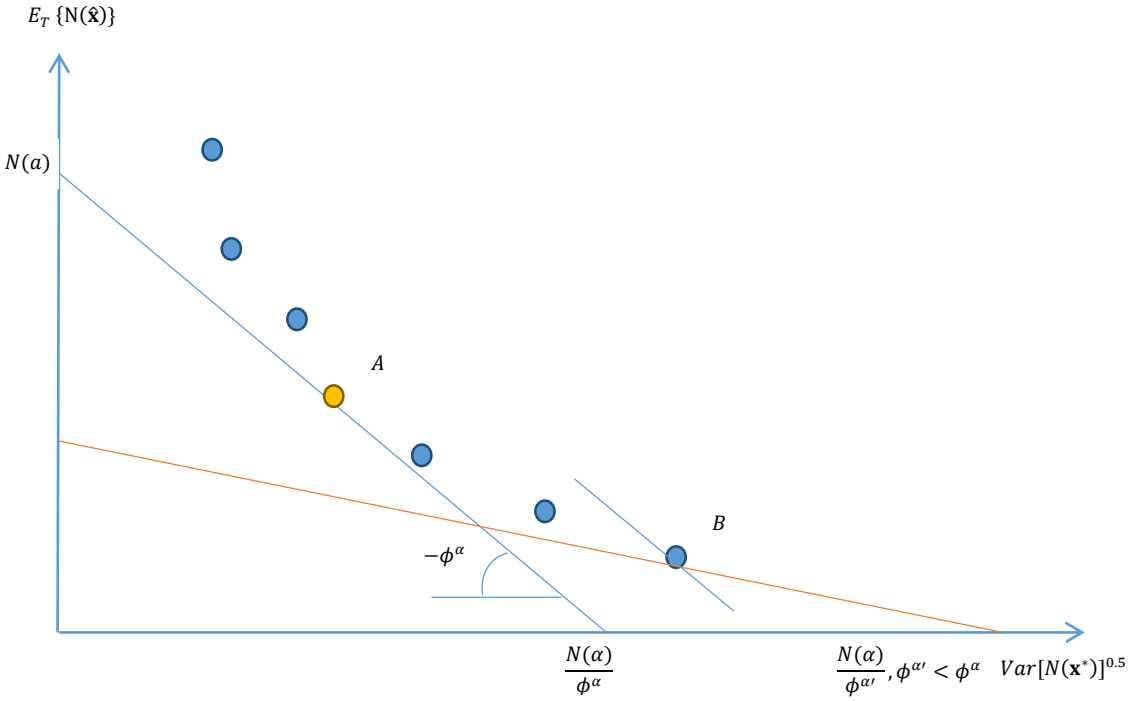
$E_T\{\mathrm{N}(\hat{\mathbf{x}})\}$
$N(a)$
A
B
$-\phi^{\alpha}$
$\frac{N(\alpha)}{\phi^{\alpha}}$
$\frac{N(\alpha)}{\phi^{\alpha\prime}}, \phi^{\alpha\prime} < \phi^{\alpha}$
$Var[N(\mathbf{x}^*)]^{0.5}$

Figure A2 The Pareto frontrier: Cost-Mean-Standard deviation

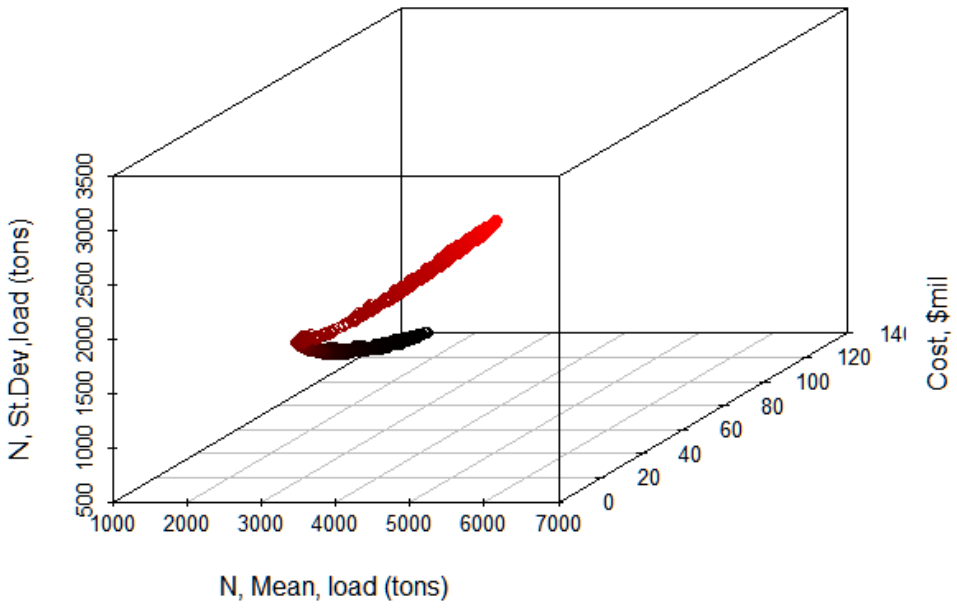

Figure A3: Distribution of Conservation Practices

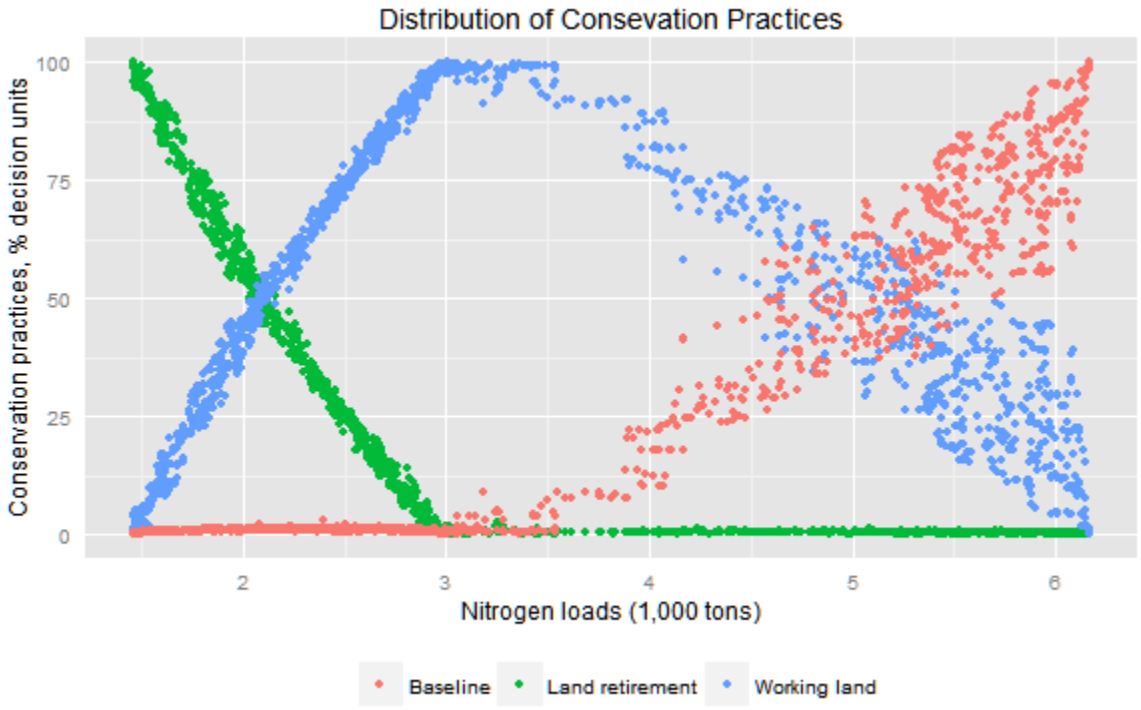

Figure A3 shows the distribution of conservation practices across the entire set of Pareto-efficient solutions expressed as the percentage of the number of decision-making units ("fields") selected to a type of conservation practice.[13]

We group cover crops, no-till and their combination into a single category labeled as "Working Land". "Baseline" represents the case where no action is taken, and "Land Retirement" considers taking land out of agricultural production. As expected, lower levels of nutrient loads can be achieved by placing land in land retirement, and larger loads correspond to using "Working Land" conservation actions.

[13] The decision-making unit in the analysis is an HRU, or a Hydrologic Response Unit (see Gassman, 2008).

The three groups each display an inflection point that corresponds approximatively to the same level of emissions. Hence, the steeper part in Figure 1(b) can be explained by the decline in the use of “Land Retirement”; the smoother decreasing part is explained by the decline in ”Working Land”, while the relatively flat area is explained by the increase in the baseline. These trends suggest that land retirement leads to lower variation in N pollution and targets with higher resilience will require using it extensively (following Gren 2010, one can say that land retirement possesses “resilience value” with respect to nutrient reductions). Similar variation-reducing properties of simulating land retirement were reported in Rabotyagov, Jha, and Campbell (2010). The inflection point can be also explained by the limited effectiveness of the “working land” practices considered in reducing N and by the fact that “Land Retirement” is the most effective conservation practice. The inflection point corresponds to a low level of emissions (high level of targets), where steep increases in land retirement are needed to attain those expected reductions in N.

Figure A4 Comparison α-resilient Pareto Frontiers

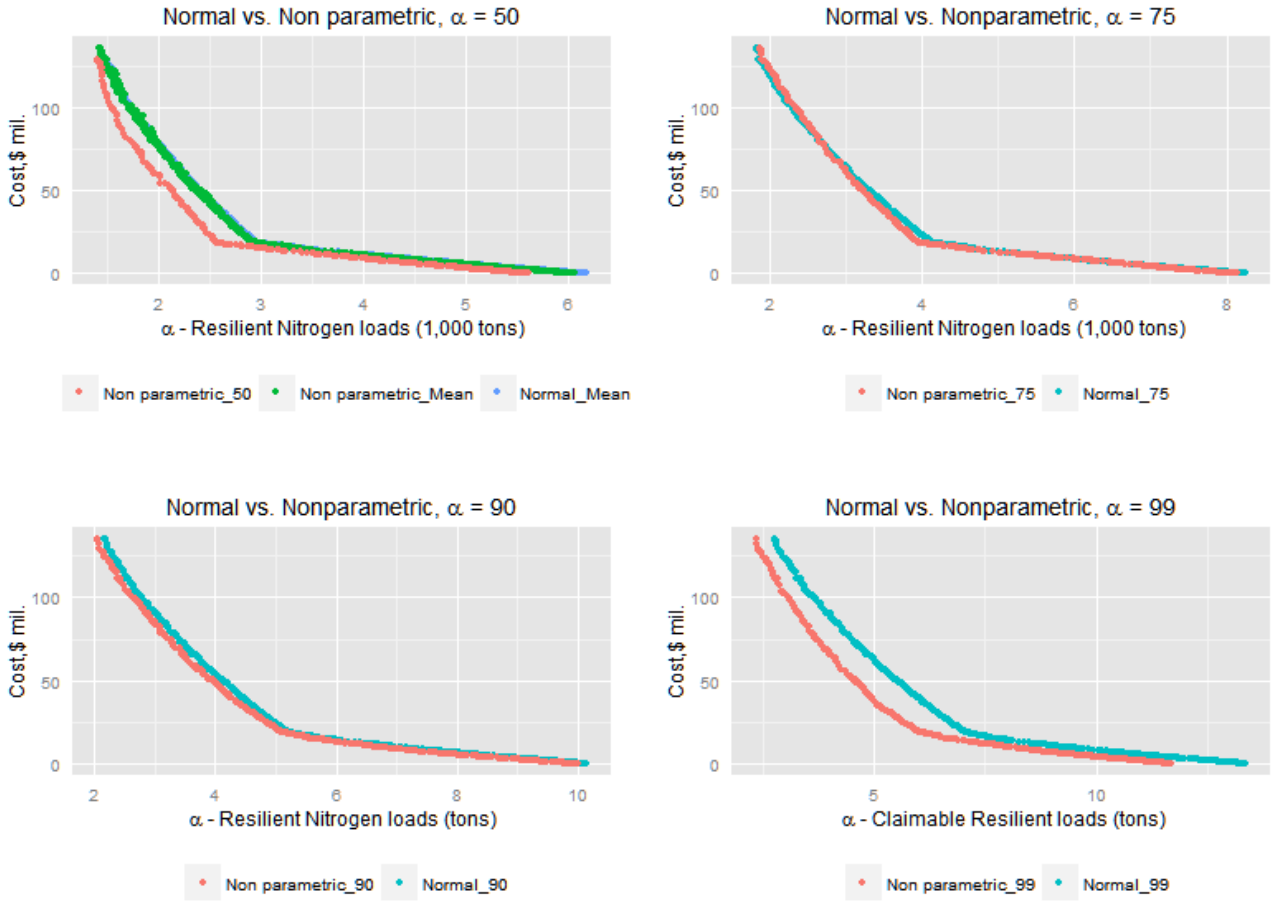

Figure A5 Cost-Resilience Trade-offs

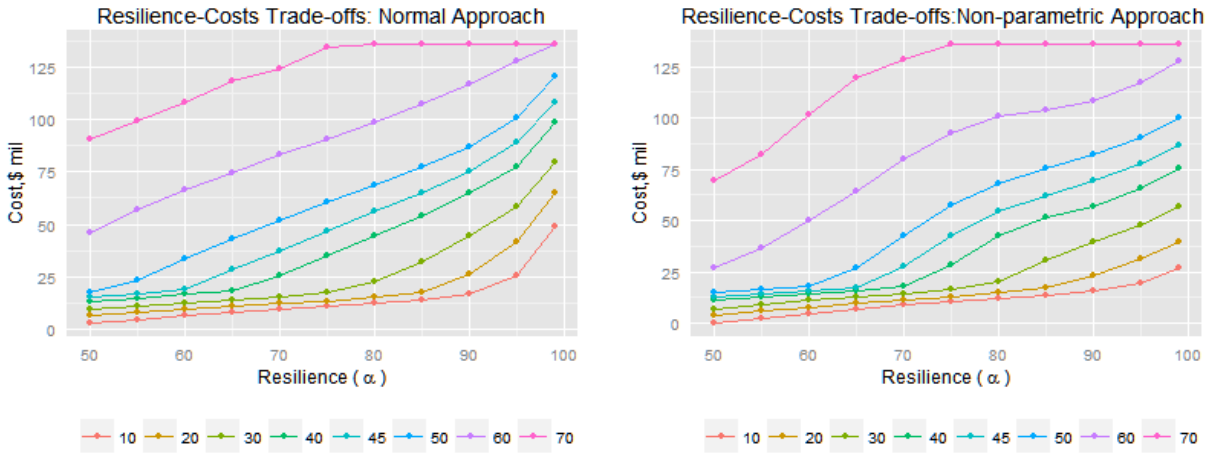

Figure A4 compares pairwise the resilient Pareto frontiers under the two approaches. The comparisons suggest that the non-parametric distribution has lighter tails than the normal distribution. This difference suggests that for a very large resilience (99), the critical value for standard normal is too conservative relative to the corresponding bootstrapped quantile. Figure A5 summarizes the resilience - cost trade-offs for achieving the same level of resilient N loads. We define a set of eight nitrogen load targets ($\overline{N}$,) each corresponding to reductions in the historical loads ranging from 10 percent to 70 percent.

Figure A6 Resilience-Nitrogen-Phosphorus Trade-offs

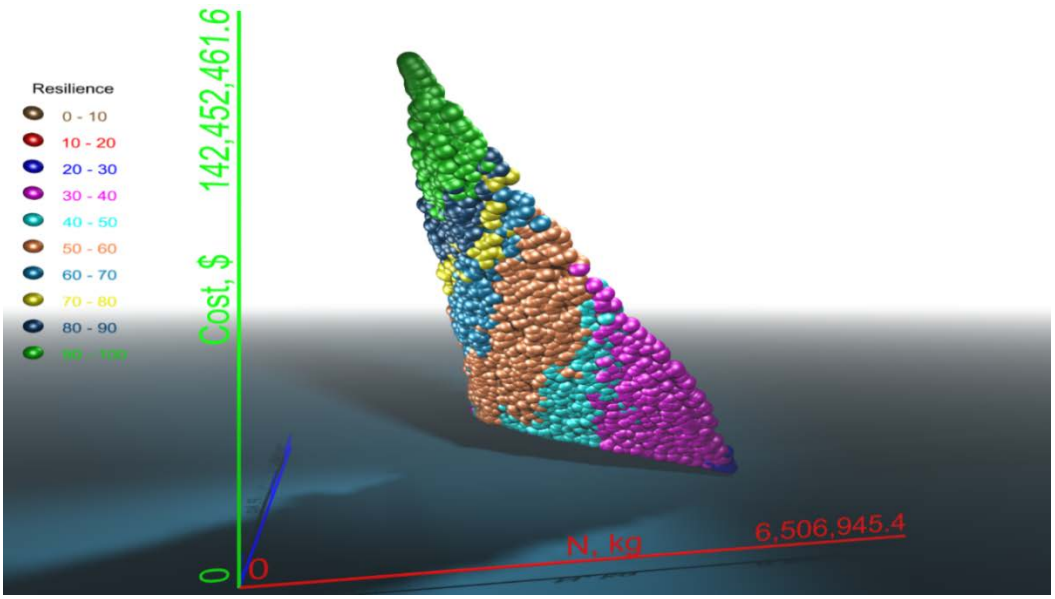

A three dimension illustration of this tradeoffs when the targets are set equal to 45 percent reductions for both N and P (equation 9) is presented in the supplemental material (Figure A6). Each element on this frontier (a 3-dimensional projection of the 5-dimensional Pareto-frontier P_f^{NP}) is assessed for a resilience (probability) level of achieving this joint target. As for the single pollutant case: securing higher level of resilience demands higher costs. Furthermore, the elements in the upper part of the curve (green colored) have the highest level of resilience (higher than 90 percent) but at the same time they have the highest total costs. From Figure 10, one can see that for a particular interval of joint resilience, there is more than one solution on the frontier. Thus, it is likely, that for a particular level of simulated joint resilience, multiple solutions would be present (for example, both a solution which over-reduces N but just reduces P to satisfy the desired P-resilience and a solution that just satisfies the criterion of joint resilience would be present). Figure A7 summarizes the results of this kind of phenomenon for

ten levels of joint resilience. Note the similarity to considerations discussed in connection with figure 1.

Figure A7 Cost of Resilience under Joint Target

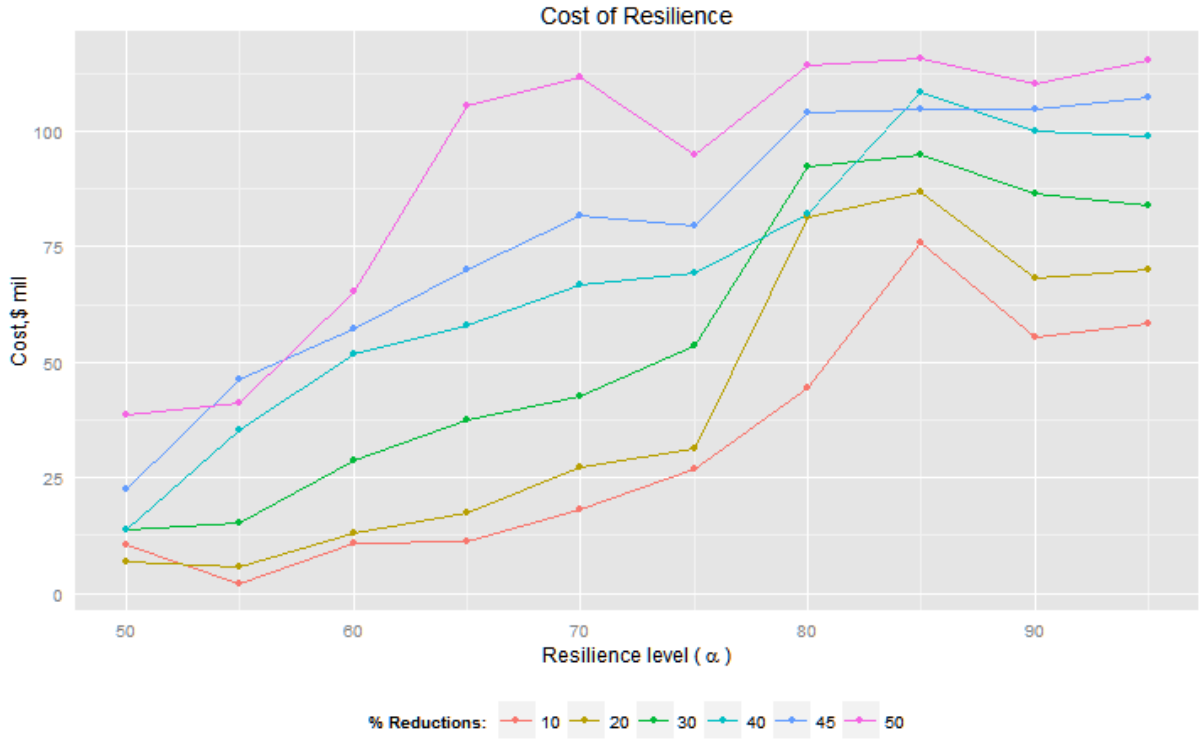

Figure A7 depicts the cost curves associated with the set of joint resilient targets. As in the single pollutant case, these curves are mostly increasing, although some of the cost curves for less stringent targets cross the cost curves for more restrictive targets, although the overlaps take place in the range of higher resilient levels. This behavior is a manifestation of inefficiencies present in the overall tradeoff frontier when evaluated from a point of view of specific nutrient reductions and their joint resilience. We conjecture that developing tailored algorithms associated with each of the lines presented would a) restore the ranking of the curves and eliminate the overlap and b) would eliminate the spikes in individual curves and therefore negative marginal costs of additional resilience.

Figure A8 Spatial Distribution of Conservation Practices in the Watershed.

A shown by our empirical findings, the distribution of conservation practices differs across resilience level. This implies that the spatial distribution will be very different. The next figures show the spatial placement of conservation practices when the target is set to 45 percent reductions and for three resilience levels: 50, 75, and 99.

Figure A8 depicts the spatial placement of the conservation practices in the watershed when the target is set equal to 45 percent reductions for N only and for joint N and P for three resilience levels: 50,75, and 99. The watershed configurations reinforce the previous findings: higher resilience levels require extensive use of land retirement, with more land retirement being used when both N and P are targeted. The non-parametric and normal watershed configurations are very similar when resilience levels are 50 or 75. However, the normal 99 resilience configuration has higher use of land retirement. This confirms the fact that the 99^{th} quantile value for the standard normal is too conservative relative to the non-parametric quantile.

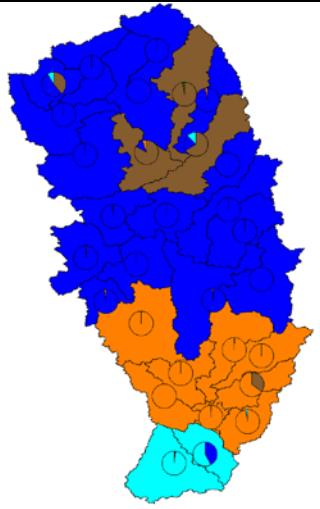 $\alpha = 50$ Non Parametric	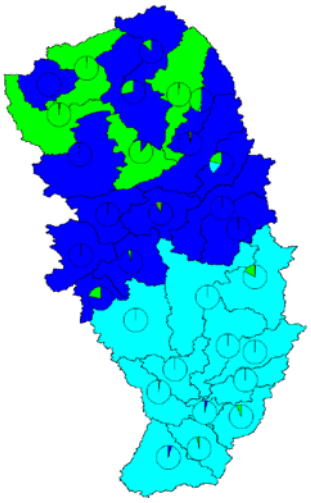 $\alpha = 75$ Non Parametric	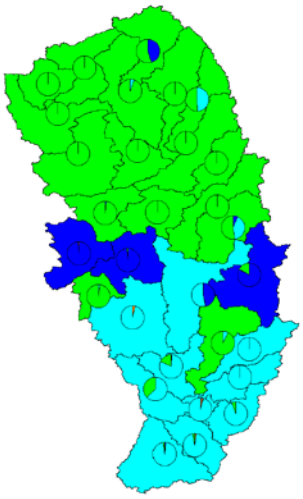 $\alpha = 99$ Non Parametric	
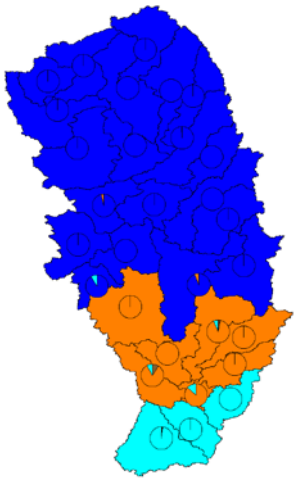 $\alpha = 50$ Normal	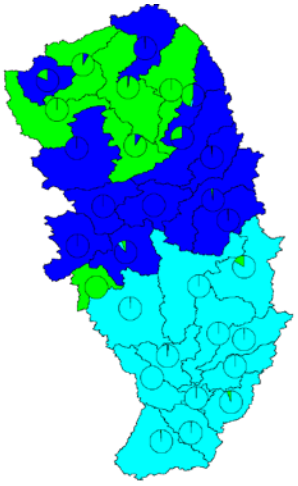 $\alpha = 75$ Normal	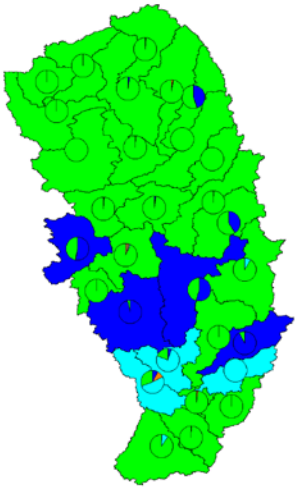 $\alpha = 99$ Normal	
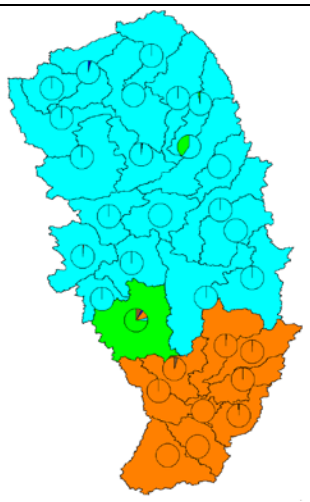 $\alpha = 50$ N and P	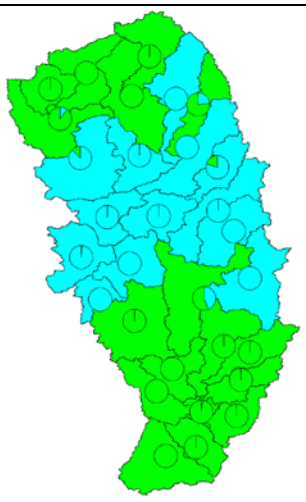 $\alpha = 75$ N and P	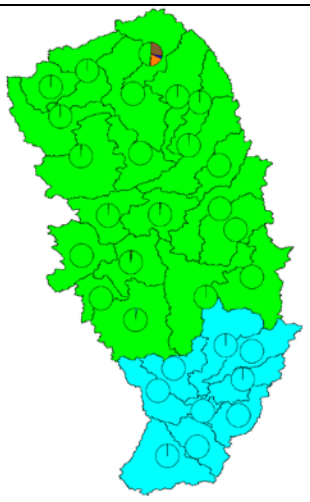 $\alpha = 99$ N and P	

Brown: Baseline; Orange: No-till; Blue: Cover Crops, Light Blue: Cover Crop and No-till, Green: Land Retirement. The main color represents the dominant color at sub-basin level. The pie charts represent percentage use for the entire set of practices[14].

[14] There are 2122 HRUs (*K* decision units). They are grouped in thirty sub-basins.

Table A1 Cost-Resilient Solutions; N reductions = 45% (target N=3.39 thousand tons N)

Resilience(α, %)	Cost (mil. $)	Marginal Cost (mil. $)	Working Land (%)	Land Retirement (%)	Baseline (%)	Cost (mil. $)	Marginal Cost (mil. $)	Working Land (%)	Land Retirement (%)	Baseline (%)
	Non-parametric					Normal				
50	12.94	0.00	91.70	0.50	7.90	15.16	0.00	99.20	0.20	0.60
55	14.47	1.52	99.20	0.20	0.60	17.08	1.92	98.30	1.00	0.80
60	16.04	1.57	96.70	0.30	3.00	19.25	2.17	98.90	0.60	0.50
65	17.61	1.57	97.90	0.20	1.90	28.36	9.11	89.80	9.50	0.80
70	27.47	9.86	93.10	5.90	1.00	37.21	8.85	78.80	20.00	1.20
75	42.40	14.93	75.50	23.20	1.20	46.89	9.68	71.40	28.00	0.60
80	54.38	11.99	63.10	35.90	1.00	56.39	9.50	64.10	35.10	0.80
85	62.06	7.68	54.40	44.60	0.90	65.27	8.88	54.90	44.20	0.90
90	69.76	7.70	48.60	50.20	1.20	75.43	10.16	44.70	54.10	1.30
95	77.54	7.78	41.20	57.80	0.90	88.93	13.50	31.50	67.60	0.90
99	86.99	9.45	40.80	58.40	0.80	107.96	19.03	17.80	81.60	0.60

Table A1 describes in detail the cost-resilient solutions for achieving the three levels of claimable nitrogen reductions for increments of about five percent increase in the resilience level from 50 to 99 probability levels for the two approaches. Column 1 shows the resilience levels α; and subsequent columns show the annual costs for achieving the required resilient loads for each level of resilience (million $), the marginal cost of achieving each additional level of resilience (million $). The following columns describe the distribution of the conservations practices: working land, land retirement and baseline (percentages of total decision-making units). We focus our analysis for case where the target is set equal to 45 percent reductions. . Resilience levels lower than 70 percent are characterized by high use of working land conservation practices

(higher than 93 percent). In order to secure higher levels of resilience more land is allocated to land retirement, but the increase takes place at a decreasing rate. For example, the use of land retirement increases from 5.9 percent (resilience level 70) to 23.2 percent (resilience level 75) (i.e. a total increase of 17 percent), but it takes only 6 additional percent to move for a resilience level of 85 to 90.

Next, we compare the costs and distribution of the conservation practices when the target is set at 45 percent reductions using normal approach with the ones described above. The total costs under the normal approach are slightly higher than under the non-parametric approach ranging from 15.94 to 107.96 million per year across different level of resilience. Lower levels of resilience are achieved by using working land conservation on a large number of fields (higher than 98 percent). Similarly, securing higher level of resilience requires putting more land in land retirement, but the use of land retirement increases at an increasing rather than decreasing rate. The increasing factor also explains the increasing trends in the marginal costs. Additionally, the optimal resilient loads ($N(\alpha)$) are a bit higher (less reductions) under the normal approach.

Table A2 Cost of Joint Resilience, 45% Reduction Target in N and P (N=3.39 thousand tons, P=0.09 thousand tons)

Resilience (α, %)	Cost (mil. $)	Marginal Cost (mil. $)	Working Land (%)	Land Retirement (%)	Baseline (%)
50	22.39	0.00	97.64	1.23	1.13
55	46.23	23.84	71.58	26.20	2.21
60	57.18	10.95	62.16	36.66	1.18
65	69.96	12.78	54.71	42.27	3.02
70	81.67	11.72	37.23	59.38	3.39
75	79.54	-2.13	44.16	55.75	0.09
80	103.92	24.37	22.48	76.34	1.18
85	104.99	1.07	21.54	77.43	1.04
90	104.72	-0.27	23.61	75.59	0.80
95	107.38	2.67	29.59	69.70	0.71